LIMNOLOGY AND OCEANOGRAPHY
ASLO
Association for the Sciences of Limnology and Oceanography

# Spatial dynamics of animal-mediated nutrients in temperate waters

| | |
|---|---|
| Journal: | *Limnology and Oceanography* |
| Manuscript ID | Draft |
| Wiley - Manuscript type: | Research Article |
| Date Submitted by the Author: | n/a |
| Complete List of Authors: | Lim, Em; Simon Fraser University Faculty of Science, Department of Biological Sciences; Bamfield Marine Sciences Centre<br>Attridge, Claire; Simon Fraser University Faculty of Science, Department of Biological Sciences<br>Cox, Kieran; Simon Fraser University Faculty of Science, Department of Biological Sciences<br>Schuster, Jasmin; Bamfield Marine Sciences Centre; University of Victoria Faculty of Science, Department of Biology; Hakai Institute<br>Kattler, Kiara; Simon Fraser University Faculty of Science, Department of Biological Sciences<br>Leedham, Emily; The University of Auckland Institute of Marine Science<br>Maher, Bridget; University of Victoria Faculty of Science, Department of Biology<br>Bickell, Andrew; Simon Fraser University Faculty of Science, Department of Biological Sciences<br>Juanes, Francis; University of Victoria Faculty of Science, Department of Biology<br>Côté, Isabelle; Simon Fraser University Faculty of Science, Department of Biological Sciences |
| Keywords: | Excretion, Consumer-mediated nutrient cycling, Nitrogen, Kelp forest, Rocky reef, Bottom-up effects, Coastal marine ecosystems |
| Abstract: | Consumer-mediated nutrient dynamics (CND), through which animals' metabolic waste products fertilize primary producers, drive variability in nutrient availability in tropical waters. This variability influences primary productivity and community functioning. Yet, examinations of CND as a driver of nutrient variability in temperate marine ecosystems are limited. Therefore, we assessed the existence and drivers of variation in CND in temperate waters at meso, small, and fine spatial scales. To do so, we quantified the occurrence of 48 fish and 92 macroinvertebrate taxa and measured in situ ammonium at 27 northeast Pacific rocky reefs for three years and 17 kelp forests of varying density for one year. Ammonium concentrations ranged from 0.01 to 2.5 uM across rocky reefs separated by tens of km. The relationship between animal abundance and ammonium among sites was mediated by water flow, where flood tides seemed to "wash away" the effect of nutrient regeneration by animals, although enrichment was possible on ebb tides. Ammonium was significantly higher within than outside of kelp forests, a difference that |

| | |
|---|---|
| | increased with kelp biomass, tide exchange, and to a lesser degree animal biomass. Caging experiments revealed that fine-scale (~2 m) ammonium variability and nutrient enrichment were only possible under low-flow conditions. Our results suggest that CND drives nutrient variability at scales ranging from two meters to over 20 km, acting on a finer scale than allochthonous nitrogen sources such as upwelling. Therefore, consumer-mediated nutrient dynamics are implicated as a previously overlooked driver of spatial variation in primary productivity in temperate marine systems. |
| | |

Scientific Significance Statement Topic

We investigated the drivers of variability in marine animal-mediated nutrients at three spatial scales. At scales of 10s of km, ammonium varied up to 16-fold across 27 rocky reefs, a larger difference than previously reported. The effect of reef-associated animal abundance on ammonium was positive but mediated by tidal exchange. At a smaller scale, ammonium concentrations were higher inside than outside 16 kelp forests, and ammonium retention increased with kelp biomass, tidal exchange, and animal biomass. Finally, by caging animals in situ, fine-scale enrichment on a scale of m was possible but only when flow was limited. Overall, animal-mediated nutrient cycling contributes to meso-, small-, and fine-scale variation in nutrients even in an upwelling region. This suggests animals may contribute more to bottom-up effects through excretion than previously considered. This work is the most extensive exploration of drivers of ammonium variability in temperate ecosystems to date.

Scientific Significance Statement Outlet

The readers of L&O will find value in our paper as it combines marine ecology with oceanography and includes both physical and biological considerations. Our research broadens our understanding of aquatic systems by documenting an overlooked driver of bottom-up effects in temperate upwelling-influenced ecosystems. This focus will appeal to all those interested in or tasked with ecosystem-based management of ocean resources.

**Title:** Spatial dynamics of animal-mediated nutrients in temperate waters

**Running title:** Animals drive nutrient variability across scales

**Authors:** Em G Lim[1,2*], Claire M Attridge[1], Kieran D Cox[1], Jasmin M Schuster[2,3,4], Kiara R Kattler[1§], Emily J Leedham[1¶], Bridget Maher[3], Andrew L Bickell[1†], Francis Juanes[3], Isabelle M Côté[1]

**Affiliations:**

[1]Department of Biological Sciences, Simon Fraser University, Burnaby, British Columbia, Canada

[2]Bamfield Marine Sciences Center, Bamfield, British Columbia, Canada

[3]Department of Biology, University of Victoria, Victoria, British Columbia, Canada

[4]Hakai Institute, Campbell River, British Columbia, Canada

[§]Present address: Department of Biological Sciences, University of Alberta, Edmonton, Canada

[¶]Present address: Institute of Marine Science, Waipapa Taumata Rau, The University of Auckland, New Zealand

[†]Present address: Department of Biology, University of Victoria, British Columbia, Canada

*Corresponding author: Em Lim, em_lim@sfu.ca

**Keywords**: Excretion, Consumer-mediated nutrient cycling, Nitrogen, Kelp forest, Rocky reef, Bottom-up effects, Coastal marine ecosystems

**Author ORCiD and contact information:**

Em G Lim: 0000-0002-3586-2108; em_lim@sfu.ca

Claire M Attridge: 0009-0007-8777-2781; claire_attridge@sfu.ca

Kieran D Cox: 0000-0001-5626-1048; kieran_cox@sfu.ca

Jasmin M Schuster: 0000-0001-8681-0757; jasmin.schuster@kelprescue.org

Kiara R Kattler: 0009-0006-4181-5945; kiara_kattler@sfu.ca

Emily J Leedham: elee323@aucklanduni.ac.nz

Bridget Maher: 0000-0002-8061-9932; bridgetmaher@uvic.ca

Andrew L Bickell: andrewbickell@uvic.ca

Francis Juanes: 0000-0001-7397-0014; juanes@uvic.ca

Isabelle M Côté: 0000-0001-5368-4061; imcote@sfu.ca

**Author Contribution Statement:**

EGL: Conceptualization (equal); formal analysis; investigation (lead); methodology (lead); visualization; writing – original draft preparation. CMA: Conceptualization (supporting); investigation (equal); methodology (equal). KDC: Conceptualization (supporting); funding acquisition (supporting); investigation (equal); methodology (equal); project administration (equal). JMS: Funding acquisition (supporting); investigation (supporting); project administration (supporting). KRK: Investigation (supporting). EJL: Investigation (supporting). BM: Investigation (supporting); methodology (supporting). ALB: Investigation (supporting). FJ: Funding acquisition (equal); project administration (supporting). IMC: Conceptualization (equal); funding acquisition (equal); methodology (equal); project administration (equal); supervision. All authors contributed to writing – review & editing.

**Abstract**

Consumer-mediated nutrient dynamics (CND), through which animals' metabolic waste products fertilize primary producers, drive variability in nutrient availability in tropical waters. This variability influences primary productivity and community functioning. Yet, examinations of CND as a driver of nutrient variability in temperate marine ecosystems are limited. Therefore, we assessed the existence and drivers of variation in CND in temperate waters at meso, small, and fine spatial scales. To do so, we quantified the occurrence of 48 fish and 92 macroinvertebrate taxa and measured in situ ammonium at 27 northeast Pacific rocky reefs for three years and 17 kelp forests of varying density for one year. Ammonium concentrations ranged from 0.01 to 2.5 uM across rocky reefs separated by tens of km. The relationship between animal abundance and ammonium among sites was mediated by water flow, where flood tides seemed to "wash away" the effect of nutrient regeneration by animals, although enrichment was possible on ebb tides. Ammonium was significantly higher within than outside of kelp forests, a difference that increased with kelp biomass, tide exchange, and to a lesser degree animal biomass. Caging experiments revealed that fine-scale (~2 m) ammonium variability and nutrient enrichment were only possible under low-flow conditions. Our results suggest that CND drives nutrient variability at scales ranging from two meters to over 20 km, acting on a finer scale than allochthonous nitrogen sources such as upwelling. Therefore, consumer-mediated nutrient dynamics are implicated as a previously overlooked driver of spatial variation in primary productivity in temperate marine systems.

## Introduction

Variation in resource availability across spatial and temporal scales can drive substantial heterogeneity in the growth, biomass and composition of primary producers (Tilman 1984; Leibold 1991; Dayton et al. 1999; McInturf et al. 2019). In many marine ecosystems, community structure is regulated through bottom-up control, i.e., it depends on factors that generate variability in the resources available to lower trophic levels (Gruner et al. 2008). Although marine ecologists have historically focused on external, abiotic sources of nutrients (e.g., upwelling) as drivers of variability in nutrient availability, there is emerging evidence that consumers also contribute to bottom-up effects (Allgeier et al. 2017). Metabolic waste products (i.e., excretion and egestion) of animals fertilize primary producers via a process termed consumer-mediated nutrient dynamics (CND; Vanni, 2002). Consumers excrete metabolic waste in the form of ammonium ($NH_4^+$), which is preferentially taken up by primary producers over other forms of nitrogen like nitrate and nitrite (Lobban and Harrison 1994; Phillips and Hurd 2004). However, the ecological importance of consumer-regenerated nutrients at varied spatial scales remains unclear. Therefore, identifying the extent to which biologically relevant variation in nutrient availability contributes to heterogeneity in primary productivity remains an active area of research (Allgeier et al. 2017).

Heterogeneity in consumer habitat use greatly influences spatial and temporal variation in nutrients supplied by animal waste (Uthicke 2001; Roman and McCarthy 2010; Benkwitt et al. 2019). For example, tropical coral reefs provide habitat, shelter, and food sources that attract dense aggregations of vertebrate and invertebrate consumers which regenerate nutrients (Archer et al. 2015; Shantz et al. 2015). On a meso scale, productivity increases with proximity to reefs with high densities of fishes (Layman et al. 2016), while on a fine scale, sheltering schools of

fish increase nitrogen concentrations around individual heads of corals relative to neighboring uninhabited corals (Holbrook et al. 2008). Diurnal migrations are another source of temporal and spatial variation in consumer-regenerated nutrients, as some fishes travel away from reefs to forage at night, then return to excrete waste around their hiding spots during the day (Meyer and Schultz 1985; Francis and Côté 2018). At an even larger-scale, variation can arise from the migration of megafauna; for instance, whales transport and deposit nutrients across thousands of kilometers as they travel from their feeding to breeding grounds (Doughty et al. 2016). However, the current understanding of animal-driven spatio-temporal variability of nitrogen is drawn substantially from tropical ecosystems (Meyer et al. 1983; Holbrook et al. 2008; Allgeier et al. 2013), often overlooking productive temperate marine ecosystems.

In temperate oceans, external sources of nutrients, such as upwelling and freshwater runoff, are generally considered the dominant drivers of nitrogen variability (Dayton et al. 1999; Lønborg et al. 2021). Due to the open nature of nearshore environments, high water flow from currents, tides, and wave action are believed to limit small-scale (1 to 100 $m^2$) nutrient variation (Probyn and Chapman 1983). Therefore, research on intertidal and shallow subtidal ecosystems has traditionally focused on top-down trophic interactions as the drivers of community composition at small scales, while limiting considerations of resource limitation to large regional or continental scales (Paine 1986; Menge 1992). However, evidence suggests meso-scale (10 to 100 km; Broitman et al., 2001) variation in allochthonous nitrogen via upwelling and internal waves may contribute to bottom-up control of marine communities (Menge et al. 1997; Nielsen and Navarrete 2004; Leichter et al. 2023) and even weaken top-down control (Sellers et al. 2020). Consumer-mediated nutrient dynamics may also contribute to smaller scales of nutrient variability than previously assumed. For instance, the abundance of intertidal mussel beds has

been linked to variation in nitrogen concentrations along entire coastlines (Pfister et al. 2014), across 10s of meters (Aquilino et al. 2009), and among tidepools (fine-scale microhabitats; Bracken, 2004). Therefore, regenerated nitrogen may contribute substantially to meso-, small-, and fine-scale variation in nutrient availability, even in high-flow, upwelling-dominated nearshore coastal ecosystems.

Shallow subtidal rocky reefs and kelp forests are temperate nearshore habitats that attract dense aggregations of fishes and invertebrates, many of which are economically, ecologically, and culturally important (Steneck et al. 2002). Elevated $NH_4^+$ excretion from the concentrated biodiversity and biomass of these communities may also contribute to nutrient hotspots on small to meso scales and exceed $NH_4^+$ delivery from other sources (Shrestha et al. 2024). Fast-growing canopy kelps, which form expansive underwater forests, may benefit from these excretions directly as a source of nitrogen (in the form of $NH_4^+$), especially during low upwelling periods (Brzezinksi et al. 2013; Lees et al. 2024). These kelps, which comprise giant kelp (*Macrocystis pyrifera*) and bull kelp (*Nereocystis leutkeana*) in the northeast Pacific, also influence the hydrodynamics and hydrochemistry of seawater, both slowing water flow within the forests and generating gradients of carbon content, pH, alkalinity, and oxygen (Jackson and Winant 1983; Gaylord et al. 2007; Pfister et al. 2019). These modifications of the surrounding fluid environment by kelp forests could affect the productivity and community composition of other primary producers and contribute to small-scale spatial nutrient heterogeneity.

We aimed to quantify the contribution of animal-regenerated nitrogen to spatial variability of nutrients in a temperate, wave-swept upwelling region (Barkley Sound, British Columbia, Canada). This region is located on the traditional territories of the Huu-ay-aht Nation and comprises an archipelago of islands dotted with rocky reefs and kelp forests of

heterogeneous structure. We hypothesized that animal-regenerated nutrients contribute to variability in resource availability across three distinct spatial scales. Specifically, we predicted that $NH_4^+$ variation would be detectable at the meso-scale due to variation in animal abundance among sites. We also expected to observe variation in $NH_4^+$ concentrations at small scales (within natural sites) and fine scales (between experimental cages), but only under conditions that allow for local enrichment (e.g., low tidal exchange). To test these predictions, we measured variation in $NH_4^+$ concentrations among rocky reef sites (meso scale of ~10s of km), in and out of kelp forest sites (small scale of 5 m), and near experimentally caged consumers (fine scale of < 2 m, Fig. 1a–c). We quantified the abundance and diversity of fishes and invertebrates at each rocky reef and kelp forest site and measured kelp forest metrics and abiotic variables to explore potential drivers of variation in $NH_4^+$ concentrations. By characterizing the scale at which animal-driven nutrients vary, we hope to uncover the extent to which consumers in temperate regions structure communities not only from the top down, but also the bottom up through CND.

## Methods

### *Site description*

Barkley Sound is located in an upwelling region on the west coast of Vancouver Island, Canada. Upwelling supplies nitrates in the spring and early summer, while storms flush riverine inputs into the nearshore in the winter and spring (Pawlowicz 2017). Due to the proximity of the Bamfield Marine Sciences Centre (BMSC), this region has been a long-term focal area for studies seeking to document the response of kelps to marine heatwaves, establish ecological baselines, and unravel ecosystem dynamics (Tanasichuk 1998; Starko et al. 2022, 2024; Attridge et al. 2024). Subtidal fish communities in this region include at least 18 families including

gobies, surfperches, rockfishes, greenlings, and sculpins (E.G. Lim, unpubl.). Macroinvertebrate assemblages, which are made up of over 49 families, are dominated by sea urchins, turban snails, sea stars, sea cucumbers, and abalone (E.G. Lim, unpubl.).

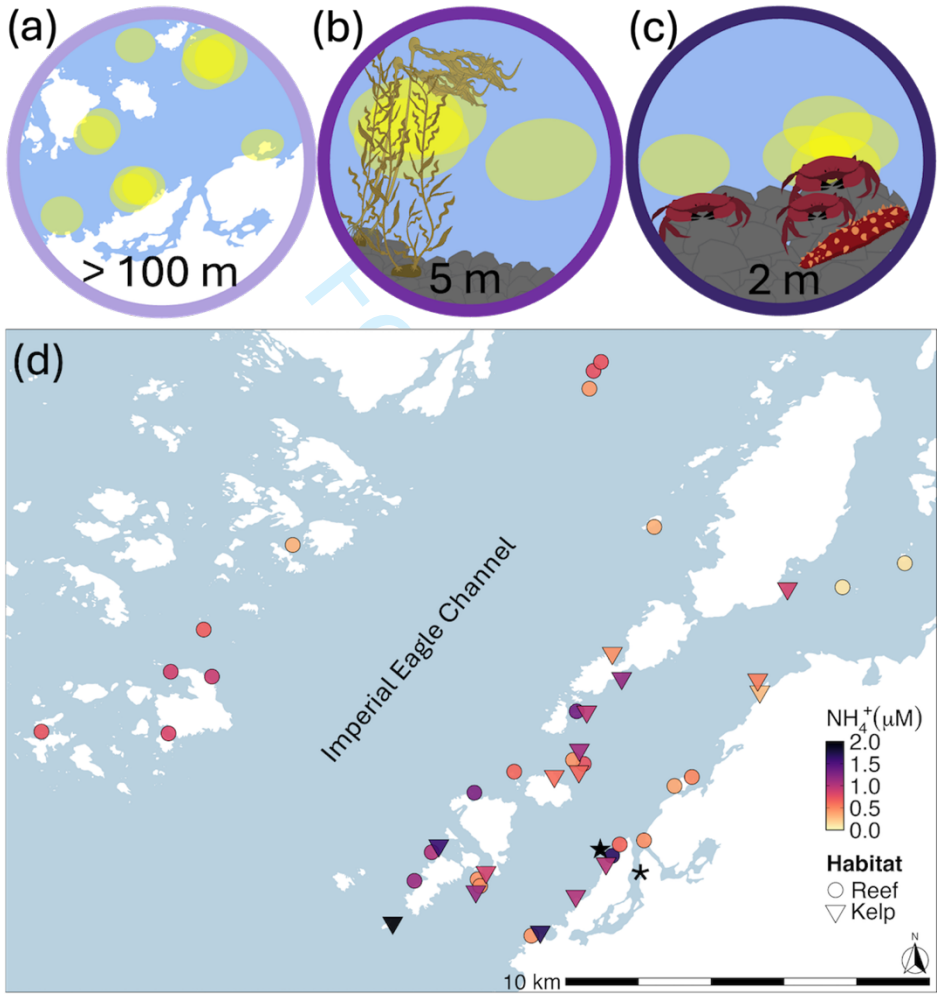


**Figure 1.** Scales of study and site locations in Barkley Sound, British Columbia, Canada. (a) Meso-scale (among-site), (b) small-scale (within-site), and (c) fine-scale (microhabitat) schematics of the three spatial scales of variability investigated. (d) Rocky reefs (circles) surveyed for meso-scale ammonium variation, and kelp forests surveyed (triangles) for small-scale ammonium variation. Site colour indicates mean ammonium concentration found at each site across all three years, with darker points having higher concentrations of ammonium. (★)

Indicates the location of the fine scale sea cucumber caging experiment and (*) denotes location of the crab caging experiment.

*Surveys of meso-scale (among-site) variation*

To explore meso-scale variation in animal-regenerated nutrients among rocky reefs, we measured ammonium ($NH_4^+$) concentrations and surveyed fish and invertebrate communities at 27 subtidal sites ranging from 0.07 – 24 km apart in Barkley Sound (Fig. 1d). We used a globally standardized method (i.e., Reef Life Survey, RLS) at each site to estimate fish and invertebrate abundance and collected subtidal $NH_4^+$ samples during each survey. We conducted our surveys in the spring (April-May) for three years (2021-2023), with all annual surveys occurring within two weeks of each other (Supplemental Material; Table S1.01). A full explanation of the Reef Life Survey method is available online (http://www.reeflifesurvey.com/methods) and provided by Edgar and Stuart-Smith (2009) and Edgar et al. (2020). Briefly, at each rocky reef site, a pair of RLS-trained SCUBA divers assessed fish and invertebrate abundance and diversity along each side of a 50 m transect line. First, fishes in the water column were counted and sized (total length, in various size class categories) within 5 m on either side of the transect line (500 $m^2$), and then benthic cryptic fishes (also sized) and large mobile invertebrates (> 2.5 cm) were counted within 1 m on either side of the transect line (100 $m^2$).

Immediately following each RLS survey, we collected three 60 mL subtidal seawater samples at 0, 25, and 50 m along the transect, 0 – 2 m above the substrate, and stored the syringes in sealed plastic bags upon collection to prevent contamination. Seawater samples were filtered into opaque amber bottles in the field and frozen for a maximum of two weeks before $NH_4^+$ analysis. We confirmed that freezing samples for this duration did not affect $NH_4^+$

194 concentration (E. G. Lim unpubl.). In 2021 and 2022, we followed the fluorometric method
195 using 40 mL seawater samples (Holmes et al. 1999), and in 2023, we followed the fluorometric
196 standard-additions protocol II (Taylor et al. 2007). These methods produce similar results,
197 although the Holmes single spike method is associated with higher variability in measurements
198 (Taylor et al. 2007). The three $NH_4^+$ samples collected during each survey were averaged to
199 determine the mean $NH_4^+$ concentration for each site.
200
201 *Surveys of small-scale (within-site) variation*
202 To investigate small-scale variation of animal-regenerated nutrients, we measured $NH_4^+$
203 concentrations inside and outside kelp forests and surveyed the resident biological communities
204 as potential moderators of this variation. Our 16 sites comprised forests of varying densities
205 dominated by giant kelp or bull kelp, and two no-kelp control sites. We conducted surveys from
206 July to September 2022 (Table S1.02). First, divers conducted RLS surveys (as above) along 50
207 m transect lines parallel to the edge of the kelp forest to quantify the abundance and biodiversity
208 of fish and invertebrate communities associated with each kelp forest. Next, divers ran four 5 m-
209 long transects perpendicular to the RLS transect (5 m apart) into the kelp forest to assess kelp
210 density, canopy height, and kelp biomass (Fig. S1.01). Divers then counted the number of
211 canopy kelp individuals (bull or giant kelp) within 0.5 m on either side of each kelp transect to
212 measure kelp density. To estimate canopy height, we measured the length of five randomly
213 selected kelp individuals per species per kelp transect; for bull kelp we measured the total length
214 from holdfast to pneumatocyst in situ, but for giant kelp, we collected five random individuals to
215 measure the length from holdfast to the tip of the apical meristem on dry land. To quantify bull
216 kelp biomass, we measured the sub-bulb circumference (15 cm below the bottom of the bulb) of

the same five bull kelps per transect in situ and calculated individual biomass using a quadratic diameter to biomass formula for Barkley Sound (C. M. Attridge unpubl.). For giant kelp biomass, we weighed (to the nearest 1 g or less) the same five individuals per transect that were collected for total length measurements. We multiplied the mean biomass estimate for each kelp species by the species density to calculate a biomass/$m^2$ estimate for each kelp transect, which we then averaged over the four transects per forest to estimate overall mean forest biomass/$m^2$. We estimated total forest area by swimming around the perimeter of the forest on the surface with a Garmin GPSMAP 78SC, which we used to calculate total forest biomass (kg).

Finally, to compare $NH_4^+$ concentrations inside vs outside each kelp forest, we collected paired 60 mL syringes of seawater immediately outside the kelp forest within 0 – 2 m above the substrate, and 5 m into the kelp forest at the same depth. We collected three paired $NH_4^+$ samples from each site, which were spaced 5 m apart, by matching them with the first three kelp transects (Fig. S1.01). Outside each kelp forest, we also filled a plastic Ziplock bag with seawater to create standards. Samples and standards were filtered into amber bottles in the field and stored on ice for transportation back to the laboratory, at which point we measured $NH_4^+$ concentration in each sample bottle following the fluorometric standard-additions protocol II for 40 mL samples (Taylor et al. 2007). For each paired inside and outside kelp forest $NH_4^+$ sample, we calculated $\Delta NH_4^+$ = inside $NH_4^+$ - outside $NH_4^+$.

*Surveys of fine-scale (microhabitat) variation*

To quantify the ability of animals to affect the $NH_4^+$ concentration in their immediate vicinity we conducted two caging experiments in situ near Bamfield, BC. We used California sea cucumbers (*Apostichopus californicus*) in the first caging experiment because they are a large, abundant

invertebrate with a high excretion rate (Bray et al. 1988). The first experiment occurred May 27 – 28, 2021 at Scott's Bay (48°50'05.2"N, 125°08'49.3"W), a wide, exposed bay that opens into Trevor Channel (Fig. 1d). We constructed 18 wire cages (26 x 26 x 26 cm), which we covered in 2 mm plastic mesh. These cages were spaced 3 m apart along two weighted lines (9 cages per line) and deployed at 3 to 5.8 m depth. We collected adult California sea cucumbers from the site via SCUBA, measured contracted sea cucumber length and girth, and immediately placed them into the cages in randomly assigned densities of 0, 1, or 2 sea cucumbers ($n$ = 6 replicates per density). After 24 hours, we returned to collect water samples from each cage in situ. While underwater, we minimized water movement by reducing our fin and hand movements while opening the mesh lids, which were secured with wire and just wide enough to collect a 60 mL syringe of seawater. Once at the surface, we filtered 40 mL of each sample into amber bottles and transported them on ice to the lab, where we measured $NH_4^+$ using the fluorometric method (Holmes et al. 1999).

We used red rock crabs (*Cancer productus*) in the second caging experiment to see if a species with an even higher individual-level excretion rate could produce fine-scale nutrient variation. The second experiment occurred over nine days from June 10 – 19, 2023 in Bamfield Inlet (48°49'53"N 125°08'11"W), a narrow, sheltered inlet (Fig. 1d). We replicated this experiment from June 19 – 28, 2023 following the same methodology. We collected red rock crabs from the site using crab traps and kept them at BMSC in flow-through sea tables for 2 – 10 days. Crabs were fed salmon every 2 – 4 days, and all crabs were fed the night before each experiment started. We constructed 12 cages from clear plastic (40 x 28 x 17 cm), with two 15 x 9 cm windows covered in a dual layer of 10 mm plastic mesh and 1 mm mesh to allow for water flow. The cages were randomly distributed every 2 m along a lead line anchored with cement

blocks 0.8 m below chart datum. Each cage contained either one large crab (carapace 15.0 – 15.9 cm), one medium crab (11.6 – 14.4 cm), or a control (i.e., a small rock, scraped clean, so weight was similar across all cages) ($n$ = 4 replicates per experiment). During both experiments, we replaced the crabs after 4 days with freshly fed, similar-sized crabs, at this point, we re-randomized the order of the cages along the line to minimize any effect of cage location. We measured seawater $NH_4^+$ concentration via snorkel at low tide at the beginning, middle, and end of each nine-day experiment. A fixed narrow rubber tube that began in the centre of the cage and extended several inches outside the mesh window allowed us to draw water samples using a 60 mL syringe without disturbing the cages. We filtered 40 mL of each sample into amber bottles, which were stored on ice before $NH_4^+$ analysis via fluorometric standard-additions protocol II (Taylor et al. 2007).

*Statistical analyses*

All statistical analysis were conducted in R (v4.1.2, R Core Team, 2019) using RStudio (v1.3.1093, RStudio Team, 2016). We used tidyverse packages for data manipulation and visualization (Wickham et al. 2019), 'glmmTMB' for all modelling (Brooks et al. 2017), and DHARMa to check model fit (Hartig 2022). We ensured all models met assumptions by inspecting residuals using the DHARMa simulateResiduals function and checked for collinearity between variables using the vif function from the car package with a cutoff value of 2.

For each Reef Life Survey conducted, we calculated fish biomass from fish length following the formula:

$$W = aL^b$$

W is fish weight, L is the fish length, a and b are species-specific constants from FishBase (Froese et al. 2014). All mobile invertebrates were counted, but only sunflower sea stars (*Pycnopodia helianthoides*) and economically important species (abalone [*Haliotis kamtschatkana*] and scallops [*Crassadoma gigantea*]) were sized. We used published length–weight relationships to calculate wet weight for these three species. For all other invertebrates, we used published wet weights to estimate biomass for each taxon. We used shell-free wet weight for species with large shells, such as hermit crabs and snails. When biomass information was unavailable for a species, we used estimates from the closest relative or most similarly sized species available (Table S1.03). Animal abundance per $m^2$ was calculated as the total number of fishes and invertebrates counted on each survey (divided by 500 $m^2$ for pelagic fishes and by 100 $m^2$ for cryptic fishes and macroinvertebrates), and we used the 'vegan' package to calculate Shannon and Simpson diversity indices (Oksanen et al. 2022). We calculated the tide exchange by computing the percent change of the tide height every minute, averaged over the hour-long survey.

Meso-scale (among-site) variation

To explore meso-scale variation in $NH_4^+$, we constructed generalized linear mixed-effect models (GLMMs) with $NH_4^+$ concentration as the response variable, and animal abundance, tide exchange, an interaction between abundance and tide, Shannon diversity, and survey depth as predictors, and random effects of site and year. All predictors were scaled and centered around the mean using the scale function. We used a gamma distribution (link = 'log'). To test the robustness of our modelling approach, we considered animal biomass as a predictor instead of abundance, and Simpson's diversity instead of Shannon diversity; alternative models including

these predictors were not better supported by AIC (Table S1.04). We ran additional models considering the effect of only the most abundant families of fishes and invertebrates, which are fully described in Supplemental Material Section 2.

Small-scale (within-site) variation

To determine whether $NH_4^+$ concentration differed inside and outside of kelp forests, we used a linear mixed-effects model (LMM) with $\Delta NH_4^+$ as the response variable ($n$ = 3 estimates per site), and kelp species, mean forest kelp biomass (per $m^2$), tide exchange, animal biomass, survey depth, Shannon diversity, and interactions between kelp biomass and tide exchange, kelp biomass and animal biomass, and animal biomass and tide exchange as fixed effects. All continuous predictors were scaled and centered around the mean as above. We included site as a random effect (1|site) as each site contributed three estimates to the analysis and used a Gaussian distribution. As above, we chose our final set of predictors upon comparing AIC values of models with alternate predictors (Table S1.05). We then ran additional models considering the effect of only the most abundant families of fishes and invertebrates (Supplemental Material Section 2).

Fine-scale (microhabitat) variation

We constructed separate linear models for each caging experiment to quantify the impact of caged animals on adjacent $NH_4^+$ concentration. For the sea cucumber experiment, we regressed cage $NH_4^+$ concentration against the treatment (i.e., sea cucumber density: 0, 1, or 2 sea cucumbers) and cage depth (centered) using a Gaussian distribution. We calculated the $NH_4^+$ excretion rate for each sea cucumber using a previously generated size-to-excretion relationship

(Table S1.06). For the red rock crab experiment, we constructed a generalized linear mixed-effects model (GLMM) with cage $NH_4^+$ concentration as the response variable and treatment (no crab, medium crab, or large crab) as the predictor variable with a gamma distribution (link = 'log'). We included a random effect of sampling day because we measured $NH_4^+$ three times per experiment, and a random effect of experimental week, because we replicated the whole experiment twice. We used a previously developed carapace-to-excretion relationship to calculate $NH_4^+$ excretion rates for each crab (Table S1.07).

**Results**

We found evidence of meso-scale variation in ammonium ($NH_4^+$) concentrations, which ranged from 0.07 µM – 2.06 µM among rocky reefs in Barkley Sound (Fig. 1d). Overall, we found no evidence that $NH_4^+$ concentration was correlated with animal abundance (GLMM, $p = 0.57$), tide exchange ($p = 0.99$), Shannon diversity ($p = 0.41$), or survey depth ($p = 0.61$; Fig. 2a; Table S1.08). However, we did find a significantly negative interaction between animal abundance and tide exchange ($p = 0.01$; Fig. 2b), revealing a weakly positive effect of total animal abundance per $m^2$ on $NH_4^+$ concentration, but only at ebb tide. In the models considering only the abundance of one animal family at a time, we found evidence for a positive relationship between the abundance of greenlings (Hexagrammidae) and whitecap limpets (Acmaeidae) and $NH_4^+$ ($p = 0.03$; Fig. S2.01). The single-family models did not reveal a significant effect of any other predictors (Fig. S2.01 and Table S2.01).

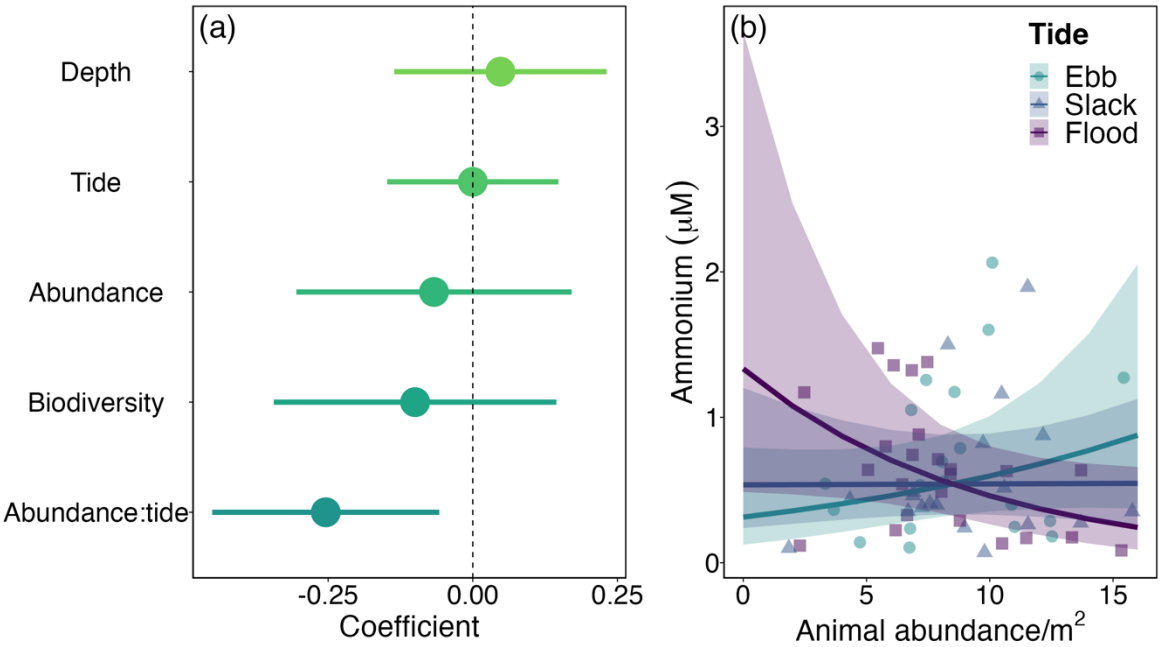


**Figure 2.** Ecological drivers of seawater ammonium concentration observed across 27 rocky reef sites (meso-scale) in Barkley Sound, British Columbia, Canada. (a) Model coefficients with 95% confidence intervals, and (b) model-generated predictions with shaded 95% confidence intervals of the effect of the interaction between animal abundance and tide exchange on among-site variation in ammonium concentration. The coefficients were generated from a generalized linear mixed-effects model with a gamma distribution (link = 'log'), so coefficients are presented in log space. Continuous predictors were centred and scaled to compare effect sizes between predictors with varying units.

We also documented evidence of significant small-scale, within-site variation of $NH_4^+$ (Fig. 3; Table S1.09).; concentrations were 1.3x higher inside giant kelp forests and 1.6x higher inside bull kelp forests than outside (LMM, $p < 0.001$; Fig. 3b). The 'excess' $NH_4^+$ concentration inside kelp forests increased with kelp biomass ($p < 0.001$; Fig. 3c), and tide exchange ($p = 0.02$;

Fig. 3a). We found limited evidence for an effect of animal biomass ($p = 0.10$; Fig. 3a), and no evidence of an effect of survey depth ($p = 0.19$; Fig. 3a), or Shannon diversity on $\Delta NH_4^+$ ($p = 0.23$; Fig. 3a). There was a positive interaction between kelp forest biomass and tide exchange, whereby the positive effect of kelp biomass on $\Delta NH_4^+$ increased with tide exchange ($p < 0.001$; Fig. 3a,c). We also identified a negative interaction between kelp biomass and animal biomass ($p = 0.04$; Fig. 3a,d), and a negative interaction between tide exchange and animal biomass ($p = 0.001$; Fig. 3a,e). The change in $NH_4^+$ was negative between samples taken 5 m apart at the no-kelp control sites ($p = 0.004$; Fig. 3b). For the single-family models, five families displayed significant relationships between biomass and $\Delta NH_4^+$, while the biomass of Gobiidae was negatively correlated with $\Delta NH_4^+$ (Fig. S2.02 and Table S2.02).

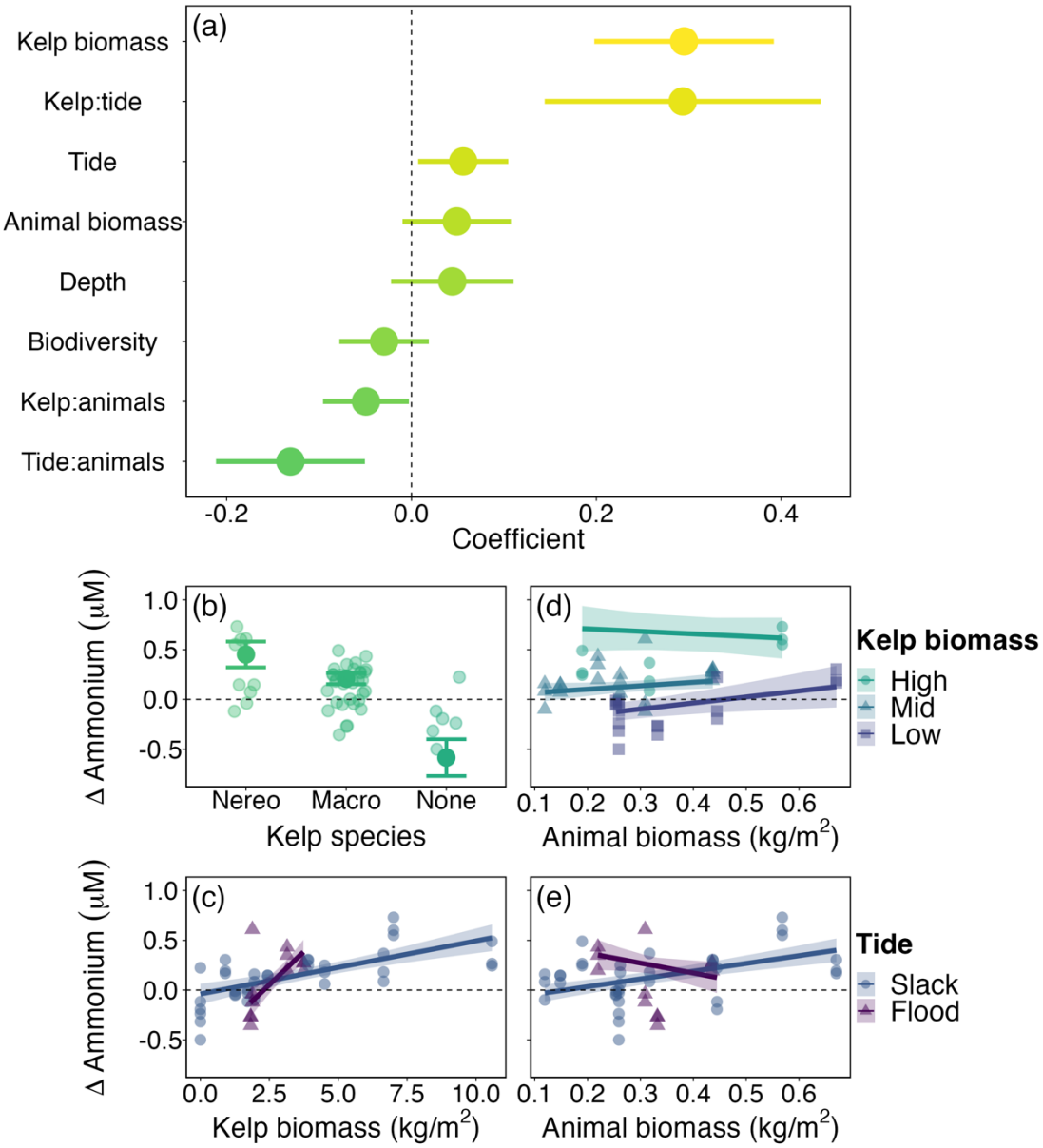


375

376 **Figure 3.** Drivers of variation in ammonium concentration inside vs outside kelp forests across
377 16 sites (small-scale) in Barkley Sound, British Columbia, Canada. (a) Model coefficients with
378 95% confidence intervals and (b-e) model-generated predictions with shaded 95% confidence
379 intervals of the effects of significant drivers of within-site variation in ammonium concentration.
380 Continuous variables were scaled and centered to facilitate comparisons between variables

381 measured in different units. Nereo = *Nereocystis luetkeana*, Macro = *Macrocystis pyrifera*, None
382 = no kelp control.
383
384 We found mixed evidence for animal-related fine-scale variability in $NH_4^+$ concentration.
385 For sea cucumbers, we found no effect of sea cucumber density on cage $NH_4^+$ concentration
386 despite a supply rate of 14 µM/h and 28 µM/h for the low and high treatments, respectively.
387 Overall, the mean $NH_4^+$ concentration was 0.92 ± 0.04 µM across all cages (LM, $p > 0.75$ for
388 both treatments; Fig. 4a; Table S1.10). However, we see a positive effect of cage depth, whereby
389 $NH_4^+$ increased by 0.38 ± 0.05 µM per m increase in depth ($p < 0.001$). For red rock crabs, both
390 medium and large crabs significantly increased the cage $NH_4^+$ concentration relative to control
391 cages, by 8.7x and 12.1x respectively (GLMM, $p < 0.001$ for all; Fig. 4b; Table S1.11). Medium
392 crabs excreted on average 88 µM/h while large crabs excreted 150 µM/h.

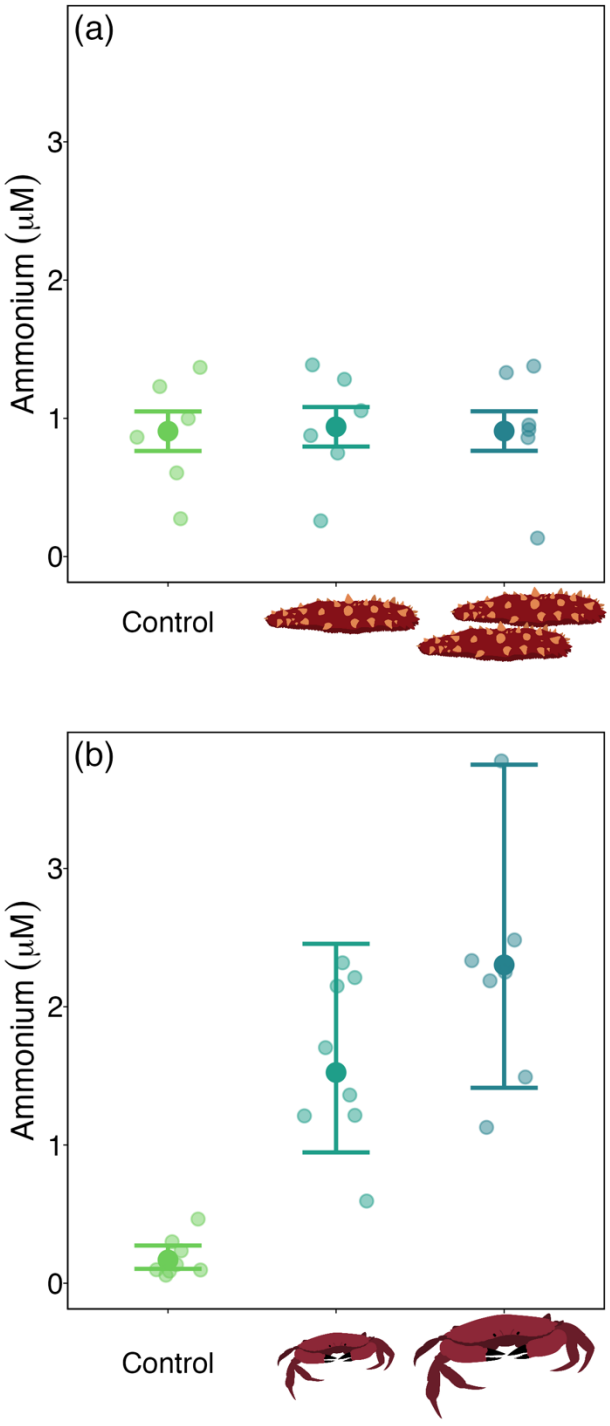




393
394 **Figure 4.** Fine scale effect of California sea cucumbers (*Apostichopus californicus*) and red rock
395 crabs (*Cancer productus*) on ammonium concentration. Mean ammonium concentration in
396 experimental cages containing (a) zero (control), one, or two California sea cucumbers ($n = 6$),

and (b) zero (control), one medium, or one large red rock crab ($n$ = 8 for control and medium, $n$ = 7 for large). Error bars indicate 95% confidence intervals.

## Discussion

We found evidence of variability of animal-regenerated nutrients from the largest to the smallest scale examined, although the strength of the signal varied. Ammonium ($NH_4^+$) varied by up to 16x between rocky reef sites within a year, 1.9x inside vs outside kelp forests, and 40x between cages with and without crabs. Water flow (i.e., tidal exchange and wave exposure) mediated the capacity for animals to saturate the water column with nutrients. Among sites a flooding tide seemed to "wash away" the impact of animals on $NH_4^+$ concentrations; in contrast, within sites, moving water made kelps' ability to slow flow and trap animal-regenerated nutrients more pronounced. In the fine-scale caging experiments we only detected an effect when the nutrient providers were crabs – an effect that we attribute mainly to the low water flow in the protected inlet rather than to the taxa. Nevertheless, across all three scales, there was animal-mediated spatial heterogeneity in nutrient availability, which may contribute to bottom-up effects.

### *Meso-scale (among-site) variation*

In rocky reef habitats, we detected a 16-fold difference in $NH_4^+$ among sites with the lowest and highest concentrations. This difference is substantially greater than previous measurements of among-site variation in nitrate (3.7x and 6.5x) and ammonium (0.4x and 0.8x) from the same region (Druehl et al. 1989; Hurd et al. 2000). It is also larger than among-site $NH_4^+$ differences measured in nearby Washington State (1.1x, Pfister et al., 2014). We had predicted that variation in $NH_4^+$ concentration among sites would be driven primarily by animal abundance. However,

the only significant predictor of among-site differences in $NH_4^+$ was a negative interaction between tide exchange and animal abundance, whereby animal excretions may enrich the seawater when the tide is ebbing, but the effect of animal abundance is washed away when the tide comes in. Although marine species diversity sometimes covaries with animal abundance or biomass (Yee and Juliano 2007; Müller et al. 2018), we found no relationship between Shannon diversity and $NH_4^+$. We did not quantify intertidal animals or microbial regeneration, which are additional sources of $NH_4^+$ (Aquilino et al. 2009; Lowman et al. 2023), but these may be more important in shallower waters and soft-sediment areas than on the subtidal rocky reefs we studied. We conclude that CND likely contributes to meso-scale variation in $NH_4^+$ in an unexpected, dynamic, tide-associated manner, which could drive among-site variation in primary productivity and thus bottom-up control.

*Small-scale (within-site) variation*

We found evidence of kelp-mediated nutrient variation on a smaller scale (5 m) than previously established. Although higher $NH_4^+$ inside high-density kelp forests has been documented (e.g., Pfister et al., 2019), these studies compared nutrient samples taken from the middle of very large kelp forests to sites more than 50 m away from the forest edges (Stewart et al. 2009; Pfister et al. 2019; Traiger et al. 2022). By sampling inside and outside forests across a gradient of kelp densities we further demonstrate a positive relationship between kelp biomass and $NH_4^+$ retention. The retention of $NH_4^+$ observed is likely due to the dampening of flow within the kelp forest bed and subsequent flow acceleration around the edges (Gaylord et al. 2007; Rosman et al. 2007). Indeed, as predicted, we found the effect of kelp biomass on $NH_4^+$ retention was more pronounced when the tide was rising (flood tide). Unfortunately, we never sampled on ebbing

443 tides, and did not quantify water motion due to waves or currents, so we could only contrast
444 slack and flooding tides. Nevertheless, it seems that water flow due to tidal exchange enhances
445 $NH_4^+$ variability within kelp forests instead of masking it.

446 We uncovered additional drivers of differences in $NH_4^+$ concentration inside and outside
447 kelp forests, namely kelp species and animal biomass. We found higher $\Delta NH_4^+$ ($NH_4^+$ inside -
448 $NH_4^+$ outside) in bull kelp forests compared to giant kelp forests, which may be due to their
449 different allocations of biomass in the water column and thus different alterations of water flow.
450 Indeed, Traiger et al., (2022) found the effect of giant kelp forests on water chemistry was
451 smaller than that of bull kelp forests, previously described by Murie and Bourdeau (2020).
452 Somewhat surprisingly, at the no kelp sites, $NH_4^+$ was lower in the "inside" samples, which were
453 closer to shore, compared to the "outside" samples, which were taken 5 m farther from shore and
454 often slightly deeper despite our efforts to maintain a consistent sampling depth. $NH_4^+$ tends to
455 *increase* with depth (Brzezinksi et al. 2013), which might explain this result. As we found the
456 opposite trend at our kelp sites, where the "inside" kelp forest samples had more $NH_4^+$ than the
457 possibly deeper "outside" samples, we are confident this result is due to retention of $NH_4^+$ by
458 kelp, instead of an artifact of our sampling procedure.

459 Even though kelp forests attract dense aggregations of fishes and invertebrates, the
460 positive effect of animal biomass on $\Delta NH_4^+$ was weak and mediated by water flow and kelp
461 biomass. Shannon diversity was positively associated with both animal and kelp biomass (Fig.
462 S1.02) but had no effect on $\Delta NH_4^+$. The negative interactions between animal biomass and both
463 tide and kelp biomass suggest a potentially saturating relationship among these variables. When
464 animal biomass was low, increased kelp biomass or tidal exchange increased $\Delta NH_4^+$, whereas at
465 high animal biomass, increasing kelp or flow had no effect. There may therefore be a threshold

for how much animals can saturate and therefore increase $\Delta NH_4^+$ in kelp forest ecosystems. Beyond this point, increased water motion or kelp biomass no longer enhances $NH_4^+$ inside kelp forests relative to the forest edge.

*Fine-scale (microhabitat) variation*

At the smallest scale of variability tested, we found evidence of variation in $NH_4^+$ only in our cage experiments in the sheltered inlet, which may suggest that water motion mediates variation at this scale as well. Under laboratory conditions we confirmed that $NH_4^+$ enrichment by animals declines with increasing flow rates (Fig. S1.03). Alternative or complementary explanations include a taxonomic effect and/or an experimental effect. The crabs in the sheltered cages excreted $NH_4^+$ at a rate roughly 6x higher than the sea cucumbers caged in the more exposed location. This difference in $NH_4^+$ production could have given us more scope to detect differences among treatments in the protected inlet. In addition, the crab cages were constructed with only two mesh windows, in contrast to the fully meshed cages of sea cucumbers, which could have promoted nutrient retention in the former. The experimental duration was also shorter for the sea cucumber experiment, but $NH_4^+$ concentrations in the crab cages were consistent across the three sampling days (day one, four, and nine) so cumulative enrichment is unlikely.

Fine-scale $NH_4^+$ enrichment by animals is nevertheless possible in wave-exposed conditions; for example, seawater above mussel beds had ~16x higher $NH_4^+$ compared to neighbouring rock without mussels on the northern California coast (Aquilino et al. 2009). Our cage experiments were not designed to test why variation was found in one experiment and not the other, but rather to see whether fine-scale variation might arise at all. Therefore, we simply

488 conclude that at least in sheltered conditions, variation on the scale of meters driven by animal
489 biomass is possible.
490
491 *Implications for primary productivity*
492 Heterogeneity in primary productivity arises from variation in resource supply. Increased
493 primary productivity has been seen with orders of variation (i.e., 1.3 – 9x) in $NH_4^+$ (Uthicke and
494 Klumpp 1998; Arzul 2001; Vinther and Holmer 2008; West et al. 2009), which is within the
495 range of variation we observed at all three spatial scales considered here. Regardless of nitrate
496 availability, $NH_4^+$ is less costly for primary producers to use, and can even inhibit nitrate uptake
497 (MacIsaac and Dugdale 1969, 1972). In nitrate-replete upwelling ecosystems of the west coast of
498 North America, a 15.8x increase in $NH_4^+$ (from 0.08 uM to 1.26 uM) was linked to increased
499 tissue nitrogen and percent cover of an intertidal seaweed (Aquilino et al. 2009), while a 1.8x
500 increase in $NH_4^+$ increased growth in subtidal seaweeds (Druehl et al. 1989). Furthermore, the
501 mismatch of timing between upwelling and the growing season at temperate latitudes leads to an
502 increased reliance on $NH_4^+$ over time as nitrate becomes depleted (Druehl et al. 1989; Brzezinksi
503 et al. 2013). For example, oceanographic processes may only provide half of the nitrogen needed
504 to sustain giant kelp growth between late summer and early fall in southern California (Fram et
505 al. 2008).
506 Heterogeneity in $NH_4^+$ availability likely influences primary productivity in Barkley
507 Sound at each spatial scale studied. Although nitrate varies among sites at the meso-scale
508 (Druehl et al. 1989; Hurd et al. 2000), external nutrient supply (upwelling) may not control
509 primary productivity as strongly as local factors (Pawlowicz 2017). The meso-scale $NH_4^+$
510 variability we documented may be one such local factor. At a small scale, nitrate from external

511 sources (e.g., upwelling and run-off) becomes depleted or unchanged as it flows through a kelp
512 forest (Pfister et al., 2019; Stewart et al., 2009), in contrast to $NH_4^+$ which is continuously
513 regenerated by animals within and around the forest and seemingly retained. As such, kelp
514 forests effectively concentrate their preferred form of nitrogen. This likely facilitates not only the
515 growth of these canopy kelps but also understory seaweeds and phytoplankton in the water
516 column. As urchin overgrazing and climate change continue to degrade kelp forests, this
517 important ecosystem function may be lost. At fine scales, invertebrates and fishes living in close
518 contact with primary producers can enrich kelps directly. Many seaweeds are capable of surge
519 uptake of $NH_4^+$ (Cedeno et al. 2021), allowing them to maximize the benefit from animal
520 excretion directly on their thalli. Indeed, given turnover rates of water and $NH_4^+$ uptake rates,
521 seaweeds in New Zealand were estimated to derive up to 79% of their needed nitrogen from
522 direct epifauna excretion (Taylor and Rees 1998).
523
524 *Conclusion*
525 Despite the mixing forces of currents, tides and waves, spatial heterogeneity in $NH_4^+$
526 concentration was detectable at meso, small, and fine spatial scales. Given the annual depletion
527 of nitrates each summer (Druehl et al. 1989), primary producers' preference for $NH_4^+$ over nitrate
528 (Phillips and Hurd 2004), and capacity for surge uptake of $NH_4^+$ (Cedeno et al. 2021), it seems
529 likely that the animal-driven variation in $NH_4^+$ we observed could be contributing to
530 heterogeneity in primary productivity. Our results disrupt the dominant paradigm that bottom-up
531 effects in temperate waters are primarily driven by external sources of nutrients acting on large
532 scales, while animals contribute to smaller-scale variation mainly through top-down,
533 consumptive effects. Instead, animals in temperate waters likely drive bottom-up effects across

multiple spatial scales while also contributing to top-down effects. Animal-driven spatio-temporal variability of nitrogen is known to drive bottom-up effects in the tropics, and our results suggest animal-regenerated nutrients also play a previously unappreciated role in shaping nutrient availability in temperate regions as well.

**Acknowledgements**

We are grateful to the volunteers who conduct annual Reef Life Surveys and to Dr. Amanda Bates and the Canada Research Chairs Program for funding this critical long-term monitoring work. Thank you to Siobhan Gray, Dave Porter, Phil Lavoie, Kelly Clement, and all the Bamfield Marine Sciences Center staff for their ongoing support. Thank you to Brittnie Spriel and Kayla Holloway for their assistance with the crab cages. Hailey Davies illustrated the red rock crabs and California sea cucumbers, and Jane Thomas provided the kelp symbols through the Integration and Application Network (ian.umces.edu/media-library). This work was funded by National Sciences and Engineering Research Council of Canada (NSERC) scholarships to EGL (CGS-M and CGS-D), CMA (CGS-M), KDC (PDF), KRK (USRA), EJL (USRA), and ALB (USRA). NSERC Discovery Grants support IMC and FJ. The Liber Ero Foundation supports FJ (Liber Ero Chair) and KDC (Liber Ero Fellow). MITACS and the Hakai Institute funding supports JMS.

**Data Availability Statement**

All datasets generated during the current study and code are available in the GitHub repository: https://github.com/em-lim13/Ch2_Spatial_pee.

## Conflict of Interest Statement

The authors declare no conflict of interest.

## References

Allgeier, J. E., D. E. Burkepile, and C. A. Layman. 2017. Animal pee in the sea: consumer-mediated nutrient dynamics in the world's changing oceans. Glob Change Biol **23**: 2166–2178. doi:10.1111/gcb.13625

Allgeier, J. E., L. A. Yeager, and C. A. Layman. 2013. Consumers regulate nutrient limitation regimes and primary production in seagrass ecosystems. Ecology **94**: 521–529. doi:https://doi.org/10.1890/12-1122.1

Aquilino, K. M., M. E. S. Bracken, M. N. Faubel, and J. J. Stachowicz. 2009. Local-scale nutrient regeneration facilitates seaweed growth on wave-exposed rocky shores in an upwelling system. Limnol Oceanogr **54**: 309–317. doi:https://doi.org/10.4319/lo.2009.54.1.0309

Archer, S. K. and others. 2015. Hot moments in spawning aggregations: implications for ecosystem-scale nutrient cycling. Coral Reefs **34**: 19–23. doi:10.1007/s00338-014-1208-4

Arzul, G. 2001. Effect of marine animal excretions on differential growth of phytoplankton species. ICES J. Mar. Sci. **58**: 386–390. doi:10.1006/jmsc.2000.1038

Attridge, C. M., K. D. Cox, B. Maher, S. Gross, E. G. Lim, K. R. Kattler, and I. M. Côté. 2024. Studying kelp forests of today to forecast ecosystems of the future. Fisheries **49**: 181–187. doi:10.1002/fsh.11065

579 Benkwitt, C. E., S. K. Wilson, and N. A. J. Graham. 2019. Seabird nutrient subsidies alter
580 patterns of algal abundance and fish biomass on coral reefs following a bleaching event.
581 Glob Change Biol **25**: 2619–2632. doi:https://doi.org/10.1111/gcb.14643
582 Bracken, M. E. S. 2004. Invertebrate-mediated nutrient loading increases growth of an intertidal
583 macroalga. J Phycol **40**: 1032–1041. doi:https://doi.org/10.1111/j.1529-
584 8817.2004.03106.x
585 Bray, R. N., A. C. Miller, S. Johnson, P. R. Krause, D. L. Robertson, and A. M. Westcott. 1988.
586 Ammonium excretion by macroinvertebrates and fishes on a subtidal rocky reef in
587 southern California. Mar. Biol. **100**: 21–30. doi:10.1007/BF00392951
588 Broitman, B. R., S. A. Navarrete, F. Smith, and S. D. Gaines. 2001. Geographic variation of
589 southeastern Pacific intertidal communities. Mar. Ecol. Prog. Ser. **224**: 21–34.
590 doi:10.3354/meps224021
591 Brooks, M. E. and others. 2017. glmmTMB balances speed and flexibility among packages for
592 zero-inflated generalized linear mixed modeling. The R Journal **9**: 378. doi:10.32614/RJ-
593 2017-066
594 Brzezinksi, M., D. Reed, S. Harrer, A. Rassweiler, J. Melack, B. Goodridge, and J. Dugan. 2013.
595 Multiple sources and forms of nitrogen sustain year-round kelp growth on the inner
596 continental shelf of the Santa Barbara Channel. Oceanog **26**: 114–123.
597 doi:10.5670/oceanog.2013.53
598 Cedeno, T. H., M. A. Brzezinski, R. J. Miller, and D. C. Reed. 2021. An evaluation of surge
599 uptake capability in the giant kelp (Macrocystis pyrifera) in response to pulses of three
600 different forms of nitrogen. Mar Biol **168**: 166. doi:10.1007/s00227-021-03975-z

601 Dayton, P. K., M. J. Tegner, P. B. Edwards, and K. L. Riser. 1999. Temporal and spatial scales
602 of kelp demography: The role of oceanographic climate. Ecol. Monogr. **69**: 219–250.
603 doi:10.1890/0012-9615(1999)069[0219:TASSOK]2.0.CO;2
604 Doughty, C. E. and others. 2016. Global nutrient transport in a world of giants. Proc Natl Acad
605 Sci USA **113**: 868–873. doi:10.1073/pnas.1502549112
606 Druehl, L. D., P. J. Harrison, K. E. Lloyd, and P. A. Thompson. 1989. Phenotypic variation in N
607 uptake by Laminaria groenlandica Rosenvinge (Laminariales, Phaeophyta). J. Exp. Mar.
608 Bio. Ecol **127**: 155–164. doi:10.1016/0022-0981(89)90181-0
609 Edgar, G. J. and others. 2020. Establishing the ecological basis for conservation of shallow
610 marine life using Reef Life Survey. Biol. Conserv. **252**: 108855.
611 doi:10.1016/j.biocon.2020.108855
612 Edgar, G., and R. Stuart-Smith. 2009. Ecological effects of marine protected areas on rocky reef
613 communities—a continental-scale analysis. Mar. Ecol. Prog. Ser. **388**: 51–62.
614 doi:10.3354/meps08149
615 Fram, J. P., H. L. Stewart, M. A. Brzezinski, B. Gaylord, D. C. Reed, S. L. Williams, and S.
616 MacIntyre. 2008. Physical pathways and utilization of nitrate supply to the giant kelp,
617 Macrocystis pyrifera. Limnol Oceanogr **53**: 1589–1603. doi:10.4319/lo.2008.53.4.1589
618 Francis, F. T., and I. M. Côté. 2018. Fish movement drives spatial and temporal patterns of
619 nutrient provisioning on coral reef patches. Ecosphere **9**: e02225. doi:10.1002/ecs2.2225
620 Froese, R., J. T. Thorson, and R. B. Reyes Jr. 2014. A Bayesian approach for estimating length-
621 weight relationships in fishes. J. Appl. Ichthyol. **30**: 78–85. doi:10.1111/jai.12299
622 Gaylord, B. and others. 2007. Spatial patterns of flow and their modification within and around a
623 giant kelp forest. Limnol Oceanogr **52**: 1838–1852. doi:10.4319/lo.2007.52.5.1838

624 Gruner, D. S. and others. 2008. A cross-system synthesis of consumer and nutrient resource
625 control on producer biomass. Ecol Lett **11**: 740–755. doi:10.1111/j.1461-
626 0248.2008.01192.x
627 Hartig, F. 2022. DHARMa: Residual diagnostics for hierarchical (multi-level / mixed) regression
628 models. R package version 0.4.6.
629 Holbrook, S. J., A. J. Brooks, R. J. Schmitt, and H. L. Stewart. 2008. Effects of sheltering fish on
630 growth of their host corals. Mar Biol **155**: 521–530. doi:10.1007/s00227-008-1051-7
631 Holmes, R. M., A. Aminot, R. Kerouel, B. A. Hooker, and B. J. Peterson. 1999. A simple and
632 precise method for measuring ammonium in marine and freshwater ecosystems. Can. J.
633 Fish. Aquat. Sci. **56**: 1801–1808. doi:https://doi.org/10.1139/f99-128
634 Hurd, C. L., K. M. Durante, and P. J. Harrison. 2000. Influence of bryozoan colonization on the
635 physiology of the kelp Macrocystis integrifolia (Laminariales, Phaeophyta) from
636 nitrogen-rich and -poor sites in Barkley Sound, British Columbia, Canada. Phycologia
637 **39**: 435–440. doi:10.2216/i0031-8884-39-5-435.1
638 Jackson, G. A., and C. D. Winant. 1983. Effect of a kelp forest on coastal currents. Continental
639 Shelf Research **2**: 75–80. doi:10.1016/0278-4343(83)90023-7
640 Layman, C. A., J. E. Allgeier, and C. G. Montaña. 2016. Mechanistic evidence of enhanced
641 production on artificial reefs: A case study in a Bahamian seagrass ecosystem. Ecol Eng
642 **95**: 574–579. doi:10.1016/j.ecoleng.2016.06.109
643 Lees, L. E., S. N. Z. Jordan, and M. E. S. Bracken. 2024. Kelps may compensate for low nitrate
644 availability by using regenerated forms of nitrogen, including urea and ammonium. J
645 Phycol **60**: 768–777. doi:10.1111/jpy.13459

646 Leibold, M. A. 1991. Biodiversity and nutrient enrichment in pond plankton communities. Evol.
647 Ecol. Res **1**: 73–95.
648 Leichter, J. J., L. B. Ladah, P. E. Parnell, M. D. Stokes, M. T. Costa, J. Fumo, and P. K. Dayton.
649 2023. Persistence of southern California giant kelp beds and alongshore variation in
650 nutrient exposure driven by seasonal upwelling and internal waves. Front. Mar. Sci. **10**.
651 doi:10.3389/fmars.2023.1007789
652 Lobban, C. S., and P. J. Harrison. 1994. Seaweed ecology and physiology, Cambridge University
653 Press.
654 Lønborg, C. and others. 2021. Nutrient cycling in tropical and temperate coastal waters: Is
655 latitude making a difference? Estuar. Coast. Shelf Sci. **262**: 107571.
656 doi:10.1016/j.ecss.2021.107571
657 Lowman, H. E., M. E. Hirsch, M. A. Brzezinski, and J. M. Melack. 2023. Examining the
658 potential of sandy marine sediments surrounding giant kelp forests to provide recycled
659 nutrients for growth. J. Coast. Res. **39**: 442–454. doi:10.2112/JCOASTRES-D-22-
660 00035.1
661 MacIsaac, J. J., and R. C. Dugdale. 1969. The kinetics of nitrate and ammonia uptake by natural
662 populations of marine phytoplankton. Deep-Sea Res. Oceanogr. Abstr. **16**: 45–57.
663 doi:10.1016/0011-7471(69)90049-7
664 MacIsaac, J. J., and R. C. Dugdale. 1972. Interactions of light and inorganic nitrogen in
665 controlling nitrogen uptake in the sea. Deep-Sea Res. Oceanogr. Abstr. **19**: 209–232.
666 doi:10.1016/0011-7471(72)90032-0

667 McInturf, A. G., L. Pollack, L. H. Yang, and O. Spiegel. 2019. Vectors with autonomy: what
668 distinguishes animal-mediated nutrient transport from abiotic vectors? Biological
669 Reviews **94**: 1761–1773. doi:10.1111/brv.12525
670 Menge, B. A. 1992. Community regulation: Under what conditions are bottom-up factors
671 important on rocky shores? Ecology **73**: 755–765. doi:10.2307/1940155
672 Menge, B. A., B. A. Daley, P. A. Wheeler, E. Dahlhoff, E. Sanford, and P. T. Strub. 1997.
673 Benthic–pelagic links and rocky intertidal communities: Bottom-up effects on top-
674 down control? Proc Natl Acad Sci USA **94**: 14530–14535. doi:10.1073/pnas.94.26.14530
675 Meyer, J. L., and E. T. Schultz. 1985. Migrating haemulid fishes as a source of nutrients and
676 organic matter on coral reefs. Limnol Oceanogr **30**: 146–156.
677 Meyer, J. L., E. T. Schultz, and G. S. Helfman. 1983. Fish schools: An asset to corals. Science
678 **220**: 1047–1049. doi:10.1126/science.220.4601.1047
679 Müller, J. and others. 2018. LiDAR-derived canopy structure supports the more-individuals
680 hypothesis for arthropod diversity in temperate forests. Oikos **127**: 814–824.
681 doi:10.1111/oik.04972
682 Murie, K. A., and P. E. Bourdeau. 2020. Fragmented kelp forest canopies retain their ability to
683 alter local seawater chemistry. Sci Rep **10**: 11939. doi:10.1038/s41598-020-68841-2
684 Nielsen, K. J., and S. A. Navarrete. 2004. Mesoscale regulation comes from the bottom-up:
685 intertidal interactions between consumers and upwelling. Ecol. Lett. **7**: 31–41.
686 doi:10.1046/j.1461-0248.2003.00542.x
687 Oksanen, J. and others. 2022. vegan: Community ecology package. R package version 2.6-4.

688 Paine, R. T. 1986. Benthic community—water column coupling during the 1982-1983 El Niño.
689 Are community changes at high latitudes attributable to cause or coincidence?1. Limnol
690 Oceanogr **31**: 351–360. doi:10.4319/lo.1986.31.2.0351
691 Pawlowicz, R. 2017. Seasonal cycles, hypoxia, and renewal in a coastal fjord (Barkley Sound,
692 British Columbia). Atmos.-Ocean **55**: 264–283. doi:10.1080/07055900.2017.1374240
693 Pfister, C. A., M. A. Altabet, and D. Post. 2014. Animal regeneration and microbial retention of
694 nitrogen along coastal rocky shores. Ecology **95**: 2803–2814. doi:10.1890/13-1825.1
695 Pfister, C. A., M. A. Altabet, and B. L. Weigel. 2019. Kelp beds and their local effects on
696 seawater chemistry, productivity, and microbial communities. Ecology **100**: e02798.
697 doi:https://doi.org/10.1002/ecy.2798
698 Phillips, J. C., and C. L. Hurd. 2004. Kinetics of nitrate, ammonium, and urea uptake by four
699 intertidal seaweeds from New Zealand. J Phycol **40**: 534–545. doi:10.1111/j.1529-
700 8817.2004.03157.x
701 Probyn, T. A., and A. R. O. Chapman. 1983. Summer growth of Chordaria flagelliformis (O.F.
702 Muell.) C. Ag.: Physiological strategies in a nutrient stressed environment. J. Exp. Mar.
703 Bio. Ecol **73**: 243–271. doi:10.1016/0022-0981(83)90050-3
704 R Core Team. 2019. R: A language and environment for statistical computing.
705 Roman, J., and J. J. McCarthy. 2010. The whale pump: Marine mammals enhance primary
706 productivity in a coastal basin P. Roopnarine [ed.]. PLoS ONE **5**: e13255.
707 doi:10.1371/journal.pone.0013255
708 Rosman, J. H., J. R. Koseff, S. G. Monismith, and J. Grover. 2007. A field investigation into the
709 effects of a kelp forest (Macrocystis pyrifera) on coastal hydrodynamics and transport. J.
710 Geophys. Res. Oceans **112**. doi:10.1029/2005JC003430

RStudio Team. 2016. RStudio: Integrated development for R.

Sellers, A. J., B. Leung, and M. E. Torchin. 2020. Global meta-analysis of how marine upwelling affects herbivory. Glob. Ecol. Biogeogr. **29**: 370–383. doi:https://doi.org/10.1111/geb.13023

Shantz, A. A., M. C. Ladd, E. Schrack, and D. E. Burkepile. 2015. Fish-derived nutrient hotspots shape coral reef benthic communities. Ecol Appl **25**: 2142–2152. doi:10.1890/14-2209.1

Shrestha, J., J. R. Peters, J. E. Caselle, and S. L. Hamilton. 2024. Marine protection and environmental forcing influence fish-derived nutrient cycling in kelp forests. Funct. Ecol. 1–15. doi:10.1111/1365-2435.14708

Starko, S. and others. 2024. Local and regional variation in kelp loss and stability across coastal British Columbia. Mar. Ecol. Prog. Ser. **733**: 1–26. doi:10.3354/meps14548

Starko, S., C. J. Neufeld, L. Gendall, B. Timmer, L. Campbell, J. Yakimishyn, L. Druehl, and J. K. Baum. 2022. Microclimate predicts kelp forest extinction in the face of direct and indirect marine heatwave effects. Ecol Appl **32**: e2673. doi:10.1002/eap.2673

Steneck, R. S., M. H. Graham, B. J. Bourque, D. Corbett, J. M. Erlandson, J. A. Estes, and M. J. Tegner. 2002. Kelp forest ecosystems: biodiversity, stability, resilience and future. Environ. Conserv. **29**: 436–459. doi:10.1017/S0376892902000322

Stewart, H., J. Fram, D. Reed, S. Williams, M. Brzezinski, S. MacIntyre, and B. Gaylord. 2009. Differences in growth, morphology and tissue carbon and nitrogen of Macrocystis pyrifera within and at the outer edge of a giant kelp forest in California, USA. Mar. Ecol. Prog. Ser. **375**: 101–112. doi:10.3354/meps07752

732 Tanasichuk, R. 1998. Interannual variations in the population biology and productivity of
733 Euphausia pacifica in Barkley Sound, Canada, with special reference to the 1992 and
734 1993 warm ocean years. Mar. Ecol. Prog. Ser. **173**: 163–180. doi:10.3354/meps173163
735 Taylor, B. W., C. F. Keep, R. O. Hall, B. J. Koch, L. M. Tronstad, A. S. Flecker, and A. J.
736 Ulseth. 2007. Improving the fluorometric ammonium method: matrix effects, background
737 fluorescence, and standard additions. J.N. Am. Benthol. Soc. **26**: 167–177.
738 doi:10.1899/0887-3593(2007)26[167:ITFAMM]2.0.CO;2
739 Taylor, R., and T. A. V. Rees. 1998. Excretory products of mobile epifauna as a nitrogen source
740 for seaweeds. Limnol Oceanogr **43**: 600–606. doi:10.4319/lo.1998.43.4.0600
741 Tilman, G. D. 1984. Plant dominance along an experimental nutrient gradient. Ecology **65**:
742 1445–1453. doi:10.2307/1939125
743 Traiger, S. B. and others. 2022. Limited biogeochemical modification of surface waters by kelp
744 forest canopies: Influence of kelp metabolism and site-specific hydrodynamics. Limnol
745 Oceanogr **67**: 392–403. doi:10.1002/lno.11999
746 Uthicke, S. 2001. Nutrient regeneration by abundant coral reef holothurians. J. Exp. Mar. Biol.
747 Ecol. **265**: 153–170. doi:10.1016/S0022-0981(01)00329-X
748 Uthicke, S., and D. W. Klumpp. 1998. Microphytobenthos community production at a near-shore
749 coral reef: seasonal variation and response to ammonium recycled by holothurians. Mar
750 Ecol Prog Ser **169**: 1–11.
751 Vanni, M. J. 2002. Nutrient cycling by animals in freshwater ecosystems. Annu Rev Ecol Syst
752 **33**: 341–370. doi:10.1146/annurev.ecolsys.33.010802.150519

753 Vinther, H. F., and M. Holmer. 2008. Experimental test of biodeposition and ammonium
754 excretion from blue mussels (Mytilus edulis) on eelgrass (Zostera marina) performance.
755 J. Exp. Mar. Bio. Ecol **364**: 72–79. doi:10.1016/j.jembe.2008.07.003
756 West, E. J., K. A. Pitt, D. T. Welsh, K. Koop, and D. Rissik. 2009. Top-down and bottom-up
757 influences of jellyfish on primary productivity and planktonic assemblages. Limnol
758 Oceanogr **54**: 2058–2071. doi:https://doi.org/10.4319/lo.2009.54.6.2058
759 Wickham, H. and others. 2019. Welcome to the tidyverse. JOSS **4**: 1686.
760 doi:10.21105/joss.01686
761 Yee, D. A., and S. A. Juliano. 2007. Abundance matters: a field experiment testing the more
762 individuals hypothesis for richness–productivity relationships. Oecologia **153**: 153–162.
763 doi:10.1007/s00442-007-0707-1
764
765

**Supplemental Material for:**

**Title:** Spatial dynamics of animal-mediated nutrients in temperate waters

**Authors:** Em G Lim[1,2*], Claire M Attridge[1], Kieran D Cox[1], Jasmin M Schuster[2,3,4], Kiara R Kattler[1§], Emily J Leedham[1¶], Bridget Maher[3], Andrew L Bickell[1†], Francis Juanes[3], Isabelle M Côté[1]

**Affiliations:**

[1]Department of Biological Sciences, Simon Fraser University, Burnaby, British Columbia, Canada

[2]Bamfield Marine Sciences Center, Bamfield, British Columbia, Canada

[3]Department of Biology, University of Victoria, Victoria, British Columbia, Canada

[4]Hakai Institute, Campbell River, British Columbia, Canada

[§]Present address: Department of Biological Sciences, University of Alberta, Edmonton, Canada

[¶]Present address: Institute of Marine Science, Waipapa Taumata Rau, The University of Auckland, New Zealand

[†]Present address: Department of Biology, University of Victoria, British Columbia, Canada

*Corresponding author: Em Lim, em_lim@sfu.ca

**Supplemental Material Section 1.**

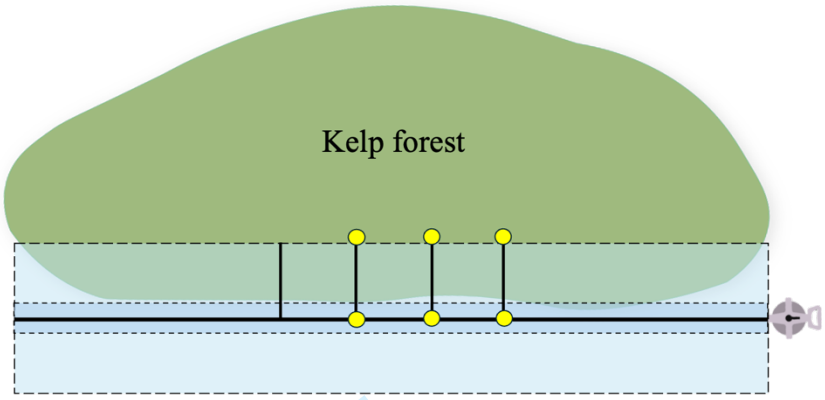


**Figure S1.01.** Schematic of methods used to survey biological communities adjacent to a kelp forest, kelp forest density, and $NH_4^+$ inside vs outside the forest. We first ran a 50 m Reef Life Survey transect parallel to the kelp forest (green shaded area) and counted fishes in the water column within 5 m on either side of the transect (light blue shaded areas), and cryptic fishes and macroinvertebrates within 1 m on either side of the transect (darker blue shaded area). Next, we ran four 5 m long transects into the kelp forest, 5 m apart from each other, to assess kelp density and biomass within 0.5 m on either side of the transect (four perpendicular black lines). Finally, we took $NH_4^+$ samples at the beginning and end of the first three kelp transects (yellow circles) to compare $NH_4^+$ inside vs outside kelp forests.

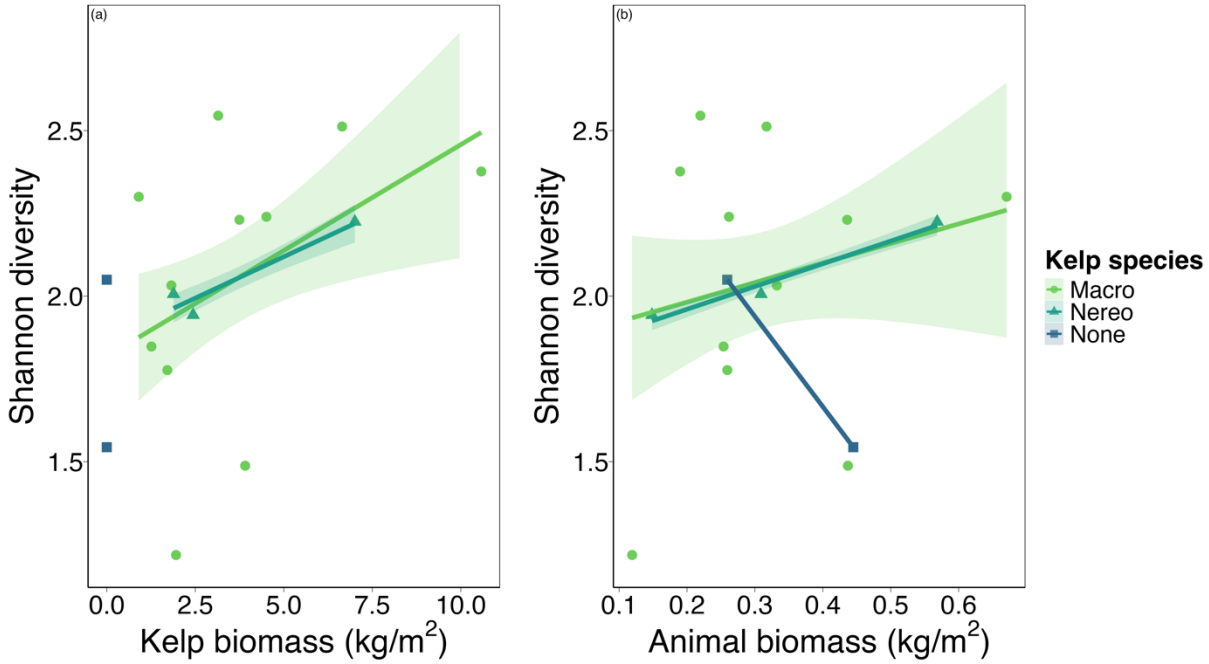


801

802 **Figure S1.02**. Relationship between Shannon diversity and (a) kelp forest biomass and (b)

803 animal biomass in kelp forests across 16 sites (small-scale) in Barkley Sound, British Columbia,

804 Canada. Macro = *Macrocystis pyrifera*, Nereo = *Nereocystis luetkeana*, None = no kelp control.

805

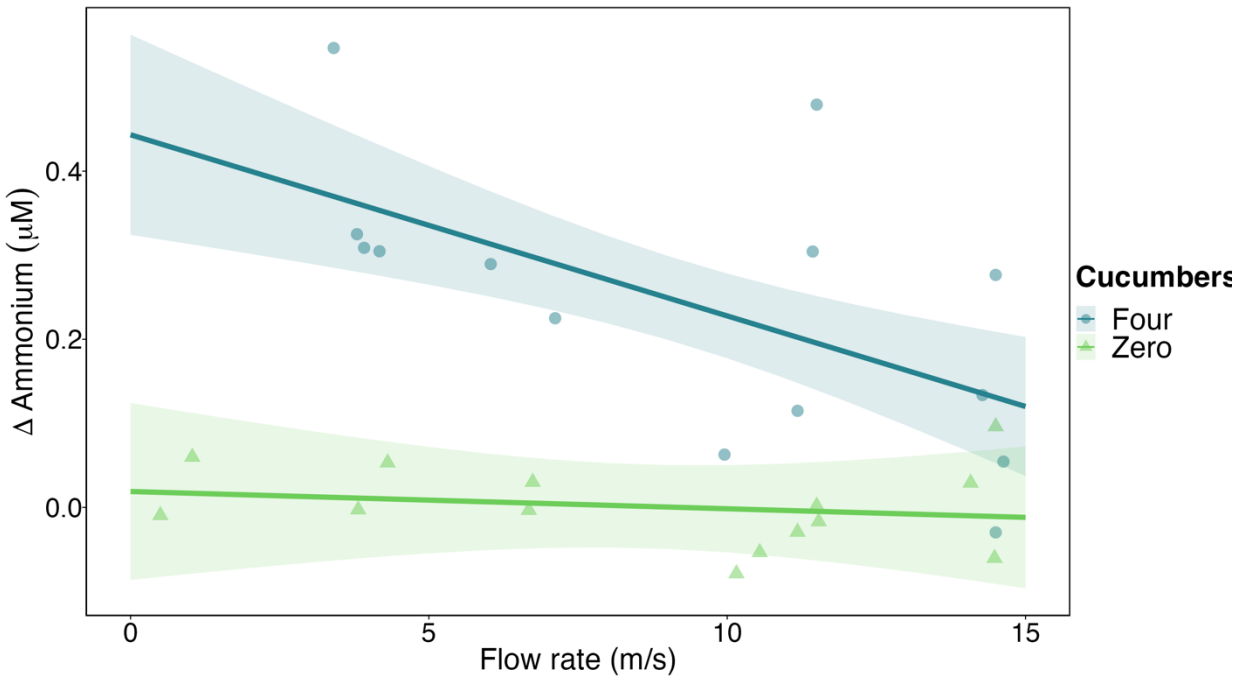


806

807 **Figure S1.03.** Change in ammonium in containers containing zero or four California sea
808 cucumbers (*Apostichopus californicus*) relative to initial ammonium concentration after 24 hours
809 in mesocosms with varying flow rates. Shaded areas indicate 95% confidence intervals, and raw
810 data are plotted as points. While $NH_4^+$ concentration remained the same across flow rates in the
811 control mesocosms, sea cucumbers enriched $NH_4^+$ concentration when flow was low. This
812 enrichment declined as flow rate increased.

813 **Table S1.01.** Rocky reef sites sampled using Reef Life Survey methods, with the associated
814 coordinates and years each site was surveyed.

| Site code | Site name | Coordinates | Years sampled |
|---|---|---|---|
| BMSC1 | Dodger Channel | 48.82894897, -125.1975708 | 2021, 2022, 2023 |
| BMSC2 | Kirby | 48.85039902, -125.1987686 | 2021, 2023 |
| BMSC3 | Ohiat | 48.85558319, -125.1837997 | 2021, 2022, 2023 |
| BMSC4 | Kii xin | 48.81511688, -125.1753311 | 2021, 2023 |
| BMSC5 | Taylor Rock | 48.82733154, -125.1966019 | 2021, 2022, 2023 |
| BMSC6 | Baeria Rocks South Island | 48.95023346, -125.1555481 | 2021, 2022, 2023 |
| BMSC7 | Baeria Rocks N Island Southside | 48.95464325, -125.1539917 | 2021 |
| BMSC8 | Baeria Rocks N Island Northside | 48.95508194, -125.1533737 | 2021, 2022, 2023 |
| BMSC9 | Eagle Bay | 48.83478928, -125.1470261 | 2021, 2022, 2023 |
| BMSC10 | Ross Islets Slug Island | 48.87051773, -125.160347 | 2021, 2022, 2023 |
| BMSC11 | Wizard Island South | 48.85746765, -125.1582336 | 2021, 2022, 2023 |
| BMSC12 | Wizard Island North | 48.858284, -125.1609192 | 2021, 2022, 2023 |
| BMSC13 | Effingham West | 48.8650322, -125.3137207 | 2021, 2022 |
| BMSC14 | Effingham Archipelago | 48.87908173, -125.2974014 | 2021, 2022 |
| BMSC15 | Raymond Kelp Rock | 48.88028336, -125.3128815 | 2021, 2022 |
| BMSC16 | Faber Islets | 48.89070129, -125.300499 | 2021, 2022 |
| BMSC17 | Wouwer Channel | 48.86548233, -125.3614807 | 2021, 2022 |
| BMSC18 | Eussen Rock | 48.91161728, -125.2670364 | 2021, 2022 |
| BMSC19 | Ed King SW Pyramid | 48.82860184, -125.2212982 | 2021, 2022, 2023 |
| BMSC20 | Ed King East | 48.83566666, -125.214798 | 2021, 2022, 2023 |
| BMSC21 | Dixon SW | 48.85205078, -125.1235657 | 2021, 2022, 2023 |
| BMSC22 | Dixon Inside | 48.85426712, -125.1170349 | 2021, 2022, 2023 |
| BMSC23 | Aguilar Point | 48.837589, -125.144145 | 2022, 2023 |
| BMSC24 | Swiss Boy | 48.916073, -125.131174 | 2023 |
| BMSC25 | Goby Town | 48.838595, -125.135015 | 2023 |
| BMSC26 | Hosie South | 48.9071, -125.037017 | 2023 |
| BMSC27 | San Jose North Island | 48.901183, -125.060433 | 2023 |

815
816

817 **Table S1.02.** Kelp forest site names, coordinates, survey dates and dominant kelp forest species.

818 Macro = giant kelp (*Macrocystis pyrifera*), Nereo = bull kelp (*Nereocystis luetkeana*).

| Site code | Site name | Coordinates | Date | Kelp |
|---|---|---|---|---|
| KCCA1 | Ross Islet Slug Island | 48.87039, -125.1599 | 2022-07-04 | Macro |
| KCCA2 | Between Scott & Brady | 48.83287, -125.1493 | 2022-07-05 | Macro |
| KCCA3 | Dodger Channel 1 | 48.83072, -125.19439 | 2022-07-06 | Macro |
| KCCA4 | Flemming 112 | 48.87868, -125.1434 | 2022-07-07 | Macro |
| KCCA6 | Less Dangerous Bay | 48.87535, -125.0915 | 2022-07-24 | None |
| KCCA7 | Ed King East Inside | 48.83608, -125.2131 | 2022-07-25 | Macro |
| KCCA9 | Wizard Islet South | 48.85728, -125.1595 | 2022-07-27 | Macro |
| KCCA12 | North Helby Rock | 48.85831, -125.1649 | 2022-08-03 | Macro |
| KCCA14 | Danvers Danger Rock | 48.877, -125.0923 | 2022-08-06 | Macro |
| KCCA15 | Cable Beach | 48.82484, -125.16067 | 2022-08-07 | Nereo |
| KCCA16 | Tzartus 116 | 48.90084, -125.0811 | 2022-08-18 | Macro |
| KCCA17 | Turf Island 2 | 48.884864, -125.146937 | 2022-08-20 | Macro |
| KCCA18 | Second Beach | 48.815969, -125.174 | 2022-08-21 | Nereo |
| KCCA19 | Wizard Islet North | 48.85916, -125.15908 | 2022-08-22 | None |
| KCCA21 | Bordelais Island | 48.81822, -125.2294516 | 2022-09-01 | Nereo |
| KCCA22 | Taylor Rock | 48.82721, -125.19717 | 2022-09-05 | Macro |

819

820

821 **Table S1.03**. Wet weight estimates for each invertebrate species used to calculate total biomass
822 for Reef Life Survey data. We used shell-free wet weight for species with large shells (e.g.,
823 hermit crabs, snails). When weight information was unavailable for a species, we used estimates
824 from the closest relative or most similarly sized species available. For the three species we sized
825 in situ (*Pycnopodia helianthoides*, *Crassadoma gigantea*, and *Haliotis kamtschatkana*), we used
826 published length-weight relationships to calculate wet weight from size.

| Species | Weight (g) | Source, proxy species if applicable |
|---|---|---|
| *Cancer productus* | 200 | E.G. Lim, unpubl. |
| *Glebocarcinus oregonensis* | 3 | Hines 1982, small crabs |
| *Romaleon antennarium* | 3 | Hines 1982, small crabs |
| *Chorilia longipes* | 1.235 | Hines 1982, *Pugettia richii* |
| *Pugettia foliata* | 1.235 | Hines 1982, *Pugettia richii* |
| *Pugettia gracilis* | 1.235 | Hines 1982, *Pugettia richii* |
| *Pugettia producta* | 46 | Hines 1982 |
| *Pugettia richii* | 1.235 | Hines 1982 |
| *Scyra acutifrons* | 2 | Hines 1982 |
| *Scyra spp.* | 1.235 | Hines 1982 |
| *Cryptolithodes sitchensis* | 3 | Hines 1982, small crabs |
| *Cryptolithodes typicus* | 3 | Hines 1982, small crabs |
| *Hapalogaster mertensii* | 65 | Stewart et al. 2015, *Phyllolithodes papillosus* |
| *Lopholithodes mandtii* | 65 | Stewart et al. 2015, *Phyllolithodes papillosus* |
| *Phyllolithodes papillosus* | 65 | Stewart et al. 2015 |
| *Oregonia gracilis* | 3 | Hines 1982, small crabs |
| *Paguroidea spp.* | 0.43 | McKinney et al. 2004, Paguroidea |
| *Pagurus beringanus* | 0.43 | McKinney et al. 2004, Paguroidea |
| *Pagurus hemphilli* | 0.43 | McKinney et al. 2004, Paguroidea |
| *Pandalus danae* | 0.11 | McKinney et al. 2004, *Palaemonetes pugio* |
| *Pandalus gurneyi* | 0.11 | McKinney et al. 2004, *Palaemonetes pugio* |
| *Pandalus spp.* | 0.11 | McKinney et al. 2004, *Palaemonetes pugio* |

| | | |
|---|---|---|
| *Pandulus spp.* | 0.11 | McKinney et al. 2004, *Palaemonetes pugio* |
| *Lophopanopeus bellus* | 3 | Hines 1982, small crabs |
| *Pachycheles pubescens* | 4.25 | Stillman and Somero 1996, *Petrolisthes spp.* |
| *Petrolisthes eriomerus* | 4.25 | Stillman and Somero 1996, *Petrolisthes spp.* |
| *Heptacarpus stylus* | 0.11 | McKinney et al. 2004, *Palaemonetes pugio* |
| Brachyura spp. | 3 | Hines 1982, small crabs |
| Unidentified shrimp | 0.11 | McKinney et al. 2004, *Palaemonetes pugio* |
| *Polyorchis penicillatus* | 0.01 | Båmstedt and Martinussen 2015, *Bolinopsis infundibulum* |
| *Mitrocoma cellularia* | 0.01 | Båmstedt and Martinussen 2015, *Bolinopsis infundibulum* |
| *Pleurobrachia bachei* | 0.01 | Båmstedt and Martinussen 2015, *Bolinopsis infundibulum* |
| *Bolinopsis infundibulum* | 0.01 | Båmstedt and Martinussen 2015 |
| *Evasterias troschelii* | 66.5 | O'Clair and Rice 1985 |
| *Leptasterias hexactis* | 5.5 | Menge 1975, *Leptasterias spp.* |
| *Leptasterias spp.* | 5.5 | Menge 1975, *Leptasterias spp.* |
| *Orthasterias koehleri* | 66.5 | O'Clair and Rice 1985, *Evasterias troschelii* |
| *Pisaster brevispinus* | 146.18 | Peters et al. 2019, Pisaster giganteus |
| *Pisaster ochraceus* | 128 | Sanford 2002 |
| *Pycnopodia helianthoides* | 0.018*size^3.13 | Lee et al. 2016 |
| *Stylasterias forreri* | 66.5 | O'Clair and Rice 1985, *Evasterias troschelii* |
| *Patiria miniata* | 26.97 | Peters et al. 2019 |
| *Henricia pumila* | 10 | Menge 1975, *Henricia spp*. |
| *Henricia spp.* | 10 | Menge 1975 |
| *Dermasterias imbricata* | 92 | Montgomery 2014 |
| *Mediaster aequalis* | 10 | Menge 1975, *Henricia spp*. |
| *Solaster dawsoni* | 486 | Montgomery 2014, *Solaster stimpsoni* |
| *Solaster stimpsoni* | 486 | Montgomery 2014 |
| *Pteraster tesselatus* | 10 | Menge 1975, *Henricia spp.* |
| *Mesocentrotus franciscanus* | 29.51 | Schuster and Bates 2023 |
| *Strongylocentrotus droebachiensis* | 20 | Stewart et al. 2015, *Strongylocentrotus polyacanthus* |
| *Strongylocentrotus purpuratus* | 20 | Stewart et al. 2015, *Strongylocentrotus polyacanthus* |
| *Apostichopus californicus* | 319.31 | Peters et al. 2019, *Apostichopus parvimensis* |
| *Chlamys hastata* | 2.5 | MacDonald et al. 1991, *Chlamys spp.* |
| *Crassadoma gigantea* | 0.038*size^2.39 | MacDonald et al. 1991 |

| | | |
|---|---|---|
| *Enteroctopus dofleini* | 137.5 | Osborn 1995, *Octopus rubescens* |
| *Octopus rubescens* | 80 | Osborn 1995 |
| *Opalia wroblewskyi* | 0.91 | Palmer 1982, *Nucella spp.* |
| *Diodora aspera* | 0.91 | Palmer 1982, *Nucella spp.* |
| *Megathura crenulata* | 0.91 | Palmer 1982, *Nucella spp.* |
| *Haliotis kamtschatkana* | 0.00058*size^3.2 | Zhang et al. 2007 |
| *Neverita lewisii* | 0.91 | Palmer 1982, *Nucella spp.* |
| *Ceratostoma foliatum* | 0.91 | Palmer 1982, *Nucella spp.* |
| *Nucella lamellosa* | 0.91 | Palmer 1982, *Nucella spp.* |
| *Armina californica* | 0.54 | McKinney et al. 2004, gastropods |
| *Cadlina luteomarginata* | 0.54 | McKinney et al. 2004, gastropods |
| *Cadlina modesta* | 0.54 | McKinney et al. 2004, gastropods |
| *Cadlina sylviaearleae* | 0.54 | McKinney et al. 2004, gastropods |
| *Coryphella verrucosa* | 0.54 | McKinney et al. 2004, gastropods |
| *Dendronotus iris* | 0.54 | McKinney et al. 2004, gastropods |
| *Dirona albolineata* | 0.54 | McKinney et al. 2004, gastropods |
| *Dirona pellucida* | 0.54 | McKinney et al. 2004, gastropods |
| *Diaulula odonoghuei* | 0.54 | McKinney et al. 2004, gastropods |
| *Diaulula sandiegensis* | 0.54 | McKinney et al. 2004, gastropods |
| *Peltodoris nobilis* | 0.54 | McKinney et al. 2004, gastropods |
| *Doris montereyensis* | 0.54 | McKinney et al. 2004, gastropods |
| *Doris odhneri* | 0.54 | McKinney et al. 2004, gastropods |
| *Antiopella fusca* | 0.54 | McKinney et al. 2004, gastropods |
| *Hermissenda crassicornis* | 0.54 | McKinney et al. 2004, gastropods |
| *Acanthodoris hudsoni* | 0.54 | McKinney et al. 2004, gastropods |
| *Acanthodoris nanaimoensis* | 0.54 | McKinney et al. 2004, gastropods |
| *Onchidoris bilamellata* | 0.54 | McKinney et al. 2004, gastropods |
| *Limacia cockerelli* | 0.54 | McKinney et al. 2004, gastropods |
| *Polycera tricolor* | 0.54 | McKinney et al. 2004, gastropods |
| *Triopha catalinae* | 0.54 | McKinney et al. 2004, gastropods |
| *Triopha modesta* | 0.54 | McKinney et al. 2004, gastropods |
| *Triopha spp.* | 0.54 | McKinney et al. 2004, gastropods |
| *Melibe leonina* | 0.54 | McKinney et al. 2004, gastropods |

| | | |
|---|---|---|
| *Tritonia festiva* | 0.54 | McKinney et al. 2004, gastropods |
| *Acmaea mitra* | 0.91 | Palmer 1982, *Nucella spp.* |
| *Lottia scutum* | 0.91 | Palmer 1982, *Nucella spp.* |
| *Berthella chacei* | 0.91 | Palmer 1982, *Nucella spp.* |
| *Calliostoma ligatum* | 0.91 | Palmer 1982, *Nucella spp.* |
| *Tegula funebralis* | 0.91 | Palmer 1982, *Nucella spp.* |
| *Pomaulax gibberosus* | 31 | Schuster and Bates 2023 |
| *Eurylepta leoparda* | 0.54 | McKinney et al. 2004, gastropods |

**Table S1.04**. Akaike's Information Criterion (AIC) values calculated for each model of ammonium concentration in relation to animal abundance (AA) or animal biomass (AB), Shannon diversity (SHD) or Simpson diversity (SID), tide exchange rate (T), depth (D), and an interaction term. RE = random effect of both site and year. k is the number of parameters in the model. The model with the lowest AIC score is the "best" model; ΔAIC is the difference in AIC score between a given model and the "best" model; AIC weight represents the probability that a model is the best model, given the data and the set of candidate models.

| **Predictors** | **k** | **AIC** | **ΔAIC** | **AIC weight** |
|---|---|---|---|---|
| AA + SHD + T + D + AA:T + RE | 9 | 45.60 | 0.00 | 0.50 |
| AA + SID + T + D + AA:T + RE | 9 | 46.09 | 0.50 | 0.39 |
| AB + SHD + T + D + AB:T + RE | 9 | 49.70 | 4.10 | 0.06 |
| AB + SID + T + D + AB:T + RE | 9 | 49.98 | 4.38 | 0.06 |

838 **Table S1.05**. Akaike's Information Criterion (AIC) values calculated for each model of delta
839 ammonium concentration in vs outside kelp forests in relation to animal abundance (AA) or
840 animal biomass (AB), Shannon diversity (SHD) or Simpson diversity (SID), kelp species (KS),
841 kelp biomass (KB), tide exchange rate (T), depth (D), and three interaction terms. RE = random
842 effect of site. k is the number of parameters in the model. The model with the lowest AIC score
843 is the "best" model; ΔAIC is the difference in AIC score between a given model and the "best"
844 model; AIC weight represents the probability that a model is the best model, given the data and
845 the set of candidate models.

| Predictors | k | AIC | ΔAIC | AIC weight |
|---|---|---|---|---|
| AB + SHD + KS + KB + T + D + AB :T + AB :KB + KB:T + RE | 13 | -33.16 | 0.00 | 0.30 |
| AA + SHD + KS + KB + T + D + AA:T + AA:KB + KB:T + RE | 13 | -32.89 | 0.27 | 0.26 |
| AA + SID + KS + KB + T + D + AA:T + AA:KB + KB:T + RE | 13 | -32.80 | 0.36 | 0.25 |
| AB + SID + KS + KB + T + D + AB:T + AB:KB + KB:T + RE | 13 | -32.38 | 0.78 | 0.20 |

846

847

848 **Table S1.06.** Excretion rate model to determine log transformed $NH_4^+$ excretion rate
849 (uM/hour/L) for California sea cucumbers (*Apostichopus californicus*) based on size index:
850 sqrt(length*girth). Adjusted R-squared for this model is 0.39.

| | Estimate | Std. error | t value | p value |
|---|---|---|---|---|
| Intercept | 1.40 | 0.22 | 6.23 | < 0.001 |
| Size index | 0.05 | 0.009 | 5.52 | < 0.001 |

851

852

853 **Table S1.07.** Excretion rate model to determine log transformed $NH_4^+$ excretion rate
854 (uM/hour/L) for red rock crabs (*Cancer productus*) based on carapace width (mm). Adjusted R-
855 squared for this model is 0.82.

| | Estimate | Std. error | t value | p value |
|---|---|---|---|---|
| Intercept | 1.22 | 0.32 | 3.76 | 0.002 |
| Carapace | 0.02 | 0.003 | 8.73 | < 0.001 |

856

857

858 **Table S1.08.** Meso-scale linear mixed-effect model describing drivers of among-site variability
859 in ammonium concentration. The model was constructed with a gamma distribution (link =
860 'log'), so coefficients are presented in log space. Continuous predictors were centred and scaled
861 to compare effect sizes between predictors with varying units.

| | Estimate | Std. error | z value | p value |
|---|---|---|---|---|
| Intercept | -0.61 | 0.25 | -2.48 | 0.01 |
| Abundance | -0.07 | 0.12 | -0.55 | 0.58 |
| Tide exchange | 0.00 | 0.08 | 0.00 | 1.00 |
| Biodiversity | -0.10 | 0.12 | -0.80 | 0.42 |
| Depth | 0.05 | 0.09 | 0.51 | 0.61 |
| Abundance:tide | -0.25 | 0.10 | -2.54 | 0.01 |

862

863

**Table S1.09**. Small-scale linear mixed effect model describing drivers of ammonium concentration inside – outside kelp forests. Continuous predictors were centred and scaled. Kelp species is a categorical predictor with three levels: macro = *Macrocystis pyrifera* (intercept level), nereo = *Nereocystis luetkeana*, none = no kelp control.

| | **Estimate** | **Std. error** | **z value** | **p value** |
|---|---|---|---|---|
| Intercept | 0.16 | 0.03 | 5.91 | < 0.001 |
| Kelp nereo | 0.24 | 0.07 | 3.64 | < 0.001 |
| Kelp none | -0.40 | 0.10 | -4.13 | < 0.001 |
| Kelp biomass | 0.29 | 0.05 | 5.95 | < 0.001 |
| Tide exchange | 0.06 | 0.02 | 2.25 | 0.02 |
| Animal biomass | 0.05 | 0.03 | 1.64 | 0.10 |
| Biodiversity | -0.03 | 0.02 | -1.20 | 0.23 |
| Depth | 0.04 | 0.03 | 1.31 | 0.19 |
| Kelp:tide | 0.29 | 0.08 | 3.85 | < 0.001 |
| Kelp:animals | -0.05 | 0.02 | -2.08 | 0.04 |
| Tide:animals | -0.13 | 0.04 | -3.19 | 0.001 |

870 **Table S1.10**. Fine-scale linear model describing ammonium variation between cages with 0, 1,
871 or 2 California sea cucumbers (*Apostichopus californicus)*.

| | Estimate | Std. error | z value | p value |
|---|---|---|---|---|
| Intercept | 0.91 | 0.07 | 12.43 | < 0.001 |
| Cukes - one | 0.03 | 0.10 | 0.31 | 0.76 |
| Cukes - two | 0.00 | 0.10 | 0.01 | 0.99 |
| Depth | 0.38 | 0.05 | 8.07 | < 0.001 |

872

873

874 **Table S1.11.** Fine-scale model describing ammonium variation between cages with zero,
875 medium, or large red rock crabs (*Cancer productus*). The model was constructed with a gamma
876 distribution (link = 'log'), so coefficients are presented in log space.

| | Estimate | Std. error | z value | p value |
|---|---|---|---|---|
| Intercept | -1.78 | 0.25 | -7.25 | < 0.001 |
| Crabs - medium | 2.20 | 0.26 | 8.48 | < 0.001 |
| Crabs - large | 2.61 | 0.27 | 9.83 | < 0.001 |

877

878

879 **References**

880 Båmstedt, U., and M. B. Martinussen. 2015. Ecology and behavior of Bolinopsis infundibulum
881 (Ctenophora; Lobata) in the Northeast Atlantic. Hydrobiologia **759**: 3–14.
882 doi:10.1007/s10750-015-2180-x
883 Hines, A. H. 1982. Allometric constraints and variables of reproductive effort in brachyuran
884 crabs. Mar. Biol. **69**: 309–320. doi:10.1007/BF00397496
885 Lee, L. C., J. C. Watson, R. Trebilco, and A. K. Salomon. 2016. Indirect effects and prey
886 behavior mediate interactions between an endangered prey and recovering predator.
887 Ecosphere **7**: e01604. doi:10.1002/ecs2.1604
888 MacDonald, B. A., R. J. Thompson, and N. F. Bourne. 1991. Growth and Reproductive
889 Energetics of three Scallop Species from British Columbia ( *Chlamys hastata* , *Chlamys*

*rubida* , and *Crassadoma gigantea* ). Can. J. Fish. Aquat. Sci. **48**: 215–221. doi:10.1139/f91-029

McKinney, R. A., S. M. Glatt, and S. R. Williams. 2004. Allometric length-weight relationships for benthic prey of aquatic wildlife in coastal marine habitats. Wildlife Biology **10**: 241–249. doi:10.2981/wlb.2004.029

Menge, B. A. 1975. Brood or broadcast? The adaptive significance of different reproductive strategies in the two intertidal sea stars Leptasterias hexactis and Pisaster ochraceus. Mar. Biol. **31**: 87–100. doi:10.1007/BF00390651

Montgomery, E. M. 2014. Predicting crawling speed relative to mass in sea stars. Journal of Experimental Marine Biology and Ecology **458**: 27–33. doi:10.1016/j.jembe.2014.05.009

O'Clair, C. E., and S. D. Rice. 1985. Depression of feeding and growth rates of the seastar Evasterias troschelii during long-term exposure to the water-soluble fraction of crude oil. Mar. Biol. **84**: 331–340. doi:10.1007/BF00392503

Osborn, S. A. 1995. Fecundity and embryonic development of Octopus rubescens Berry from Monterey Bay, California. Master of Science. San Jose State University.

Palmer, A. R. 1982. GROWTH IN MARINE GASTROPODS: A NON-DESTRUCTIVE TECHNIQUE FOR INDEPENDENTLY MEASURING SHELL AND BODY WEIGHT.

Peters, J. R., D. C. Reed, and D. E. Burkepile. 2019. Climate and fishing drive regime shifts in consumer-mediated nutrient cycling in kelp forests. Glob Change Biol **25**: 3179–3192. doi:10.1111/gcb.14706

Sanford, E. 2002. The feeding, growth, and energetics of two rocky intertidal predators (Pisaster ochraceus and Nucella canaliculata) under water temperatures simulating episodic upwelling. J. Exp. Mar. Biol. Ecol. **273**: 199–218. doi:10.1016/S0022-0981(02)00164-8

Schuster, J. M., and A. E. Bates. 2023. The role of kelp availability and quality on the energetic state and thermal tolerance of sea urchin and gastropod grazers. Journal of Experimental Marine Biology and Ecology **569**: 151947. doi:10.1016/j.jembe.2023.151947

Stewart, N. L., B. Konar, and M. T. Tinker. 2015. Testing the nutritional-limitation, predator-avoidance, and storm-avoidance hypotheses for restricted sea otter habitat use in the Aleutian Islands, Alaska. Oecologia **177**: 645–655. doi:10.1007/s00442-014-3149-6

Stillman, J. H., and G. N. Somero. 1996. Adaptation to Temperature Stress and Aerial Exposure in Congeneric Species of Intertidal Porcelain Crabs (Genus Petrolisthes): Correlation of

Physiology, Biochemistry and Morphology With Vertical Distribution. Journal of Experimental Biology **199**: 1845–1855. doi:10.1242/jeb.199.8.1845

Zhang, Z., A. Campbell, and J. Lessard. 2007. MODELING NORTHERN ABALONE, HALIOTIS KAMTSCHATKANA, POPULATION STOCK AND RECRUITMENT IN BRITISH COLUMBIA. shre **26**: 1099–1107. doi:10.2983/0730-8000(2007)26[1099:MNAHKP]2.0.CO;2

928 **Electronic Supplement Part 2.** Effect of individual families of fishes and invertebrates on
929 meso-scale (among-site) and small-scale (within-site) variation in ammonium.
930
931 **Regional (meso-scale) variation**
932 We further explored the effect of animals on variation in $NH_4^+$ concentration among rocky reef
933 sites by considering only the abundance of one animal family at a time. For each of the top 15
934 most abundant families observed on our surveys, we constructed an GLMM identical to the top
935 model shown in Table S4, using only the abundance of that family ($NH_4^+$ regressed against
936 family abundance, tide exchange, an interaction between family abundance and tide, Shannon
937 diversity, survey depth, with a random effect of site and year and a gamma distribution). Here,
938 we present the three fish families (Hexagrammidae, Gobiidae, and Sebastidae) and three
939 invertebrate families (Muricidae, Asteriidae, and Acmaeidae) with the highest $R^2$ values. These
940 six families constitute 17% of the total abundance.
941
942 We found evidence of a positive relationship between $NH_4^+$ concentration and the
943 abundance of greenlings (Hexagrammidae, GLMM, $p = 0.03$, Fig. S2.01), weak evidence of an
944 interaction between greenling abundance and tide ($p = 0.09$), but no evidence for an effect of any
945 other predictors ($p > 0.10$). We also found evidence of a positive relationship between $NH_4^+$
946 concentration and the abundance of whitecap limpets (Acmaeidae, GLMM, $p = 0.03$), but no
947 evidence of an effect of any other predictors ($p > 0.40$). We found no evidence of an effect of
948 any predictors on $NH_4^+$ concentration in the models for the families Sebastidae, Gobiidae,
949 Asteriidae, or Muricidae ($p > 0.10$). Full model outputs are available in Table S2.01.
950
951

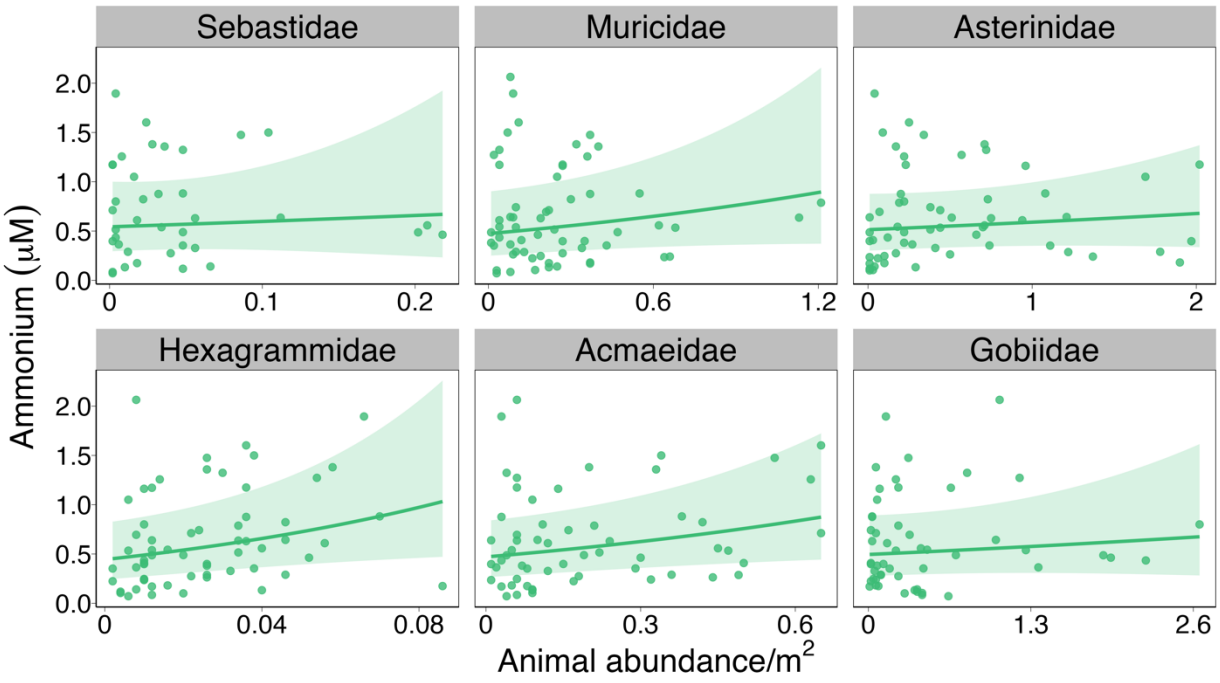


952
953 **Figure S2.01.** Model-generated predictions of ammonium concentrations in relation to
954 abundance across rocky reef sites for the 6 animal families with the highest $R^2$.

955
956 **Table S2.01.** Model summaries from the meso-scale (among-site) models including only the
957 biomass of one family (indicated in the top left cell) for each model.

958

| **Sebastidae** ($R^2$ = 0.67) | **Estimate** | **Std. error** | **z-value** | **p-value** |
|---|---|---|---|---|
| Intercept | 0.13 | 1.23 | 0.11 | 0.91 |
| Abundance | 1.98 | 3.22 | 0.61 | 0.54 |
| Tide exchange | -0.53 | 1.00 | -0.53 | 0.60 |
| Biodiversity | -0.10 | 0.13 | -0.75 | 0.45 |
| Depth | -0.02 | 0.13 | -0.18 | 0.86 |
| Abundance:tide | -1.79 | 2.82 | -0.63 | 0.53 |

959
960

| **Muricidae** ($R^2$ = 0.54) | **Estimate** | **Std. error** | **z value** | **p value** |
|---|---|---|---|---|
| Intercept | -0.43 | 0.33 | -1.30 | 0.19 |
| Abundance | 0.79 | 0.51 | 1.55 | 0.12 |
| Tide exchange | 0.05 | 0.12 | 0.44 | 0.66 |
| Biodiversity | 0.00 | 0.10 | -0.04 | 0.97 |
| Depth | 0.04 | 0.09 | 0.43 | 0.67 |
| Abundance:tide | 0.12 | 0.55 | 0.22 | 0.83 |

961

| **Asterinidae** ($R^2$ = 0.651) | **Estimate** | **Std. error** | **z value** | **p value** |
|---|---|---|---|---|
| Intercept | -0.58 | 0.26 | -2.28 | 0.02 |
| Abundance | 0.21 | 0.26 | 0.80 | 0.42 |
| Tide exchange | 0.12 | 0.07 | 1.80 | 0.07 |
| Biodiversity | -0.12 | 0.09 | -1.29 | 0.20 |
| Depth | 0.06 | 0.09 | 0.62 | 0.54 |
| Abundance:tide | 0.07 | 0.27 | 0.26 | 0.80 |

962
963

| **Hexagrammidae** ($R^2$ = 0.47) | **Estimate** | **Std. error** | **z value** | **p value** |
|---|---|---|---|---|
| Intercept | 4.96 | 2.54 | 1.95 | 0.05 |
| Abundance | 14.67 | 6.69 | 2.19 | 0.03 |
| Tide exchange | -3.35 | 2.01 | -1.67 | 0.10 |
| Biodiversity | 0.01 | 0.09 | 0.11 | 0.91 |
| Depth | 0.02 | 0.09 | 0.25 | 0.81 |
| Abundance:tide | -9.01 | 5.35 | -1.68 | 0.09 |

964
965

| **Acmaeidae** ($R^2$ = 0.46) | **Estimate** | **Std. error** | **z value** | **p value** |
|---|---|---|---|---|
| Intercept | -0.19 | 0.33 | -0.59 | 0.56 |
| Abundance | 1.42 | 0.67 | 2.13 | 0.03 |
| Tide exchange | 0.03 | 0.16 | 0.21 | 0.84 |
| Biodiversity | -0.01 | 0.09 | -0.09 | 0.93 |
| Depth | 0.00 | 0.09 | 0.05 | 0.96 |
| Abundance:tide | -0.16 | 0.58 | -0.28 | 0.78 |

966
967

| **Gobiidae** ($R^2$ = 0.44) | **Estimate** | **Std. error** | **z value** | **p value** |
|---|---|---|---|---|
| Intercept | -0.64 | 0.29 | -2.19 | 0.03 |
| Abundance | 0.17 | 0.23 | 0.75 | 0.45 |
| Tide exchange | 0.04 | 0.07 | 0.52 | 0.61 |
| Biodiversity | -0.01 | 0.10 | -0.11 | 0.91 |
| Depth | -0.06 | 0.11 | -0.55 | 0.58 |
| Abundance:tide | 0.13 | 0.17 | 0.80 | 0.43 |

968

969 **Within-site (small-scale) variation**

970 As above, we further explored the effect of animals on $\Delta NH_4^+$ – the difference in $NH_4^+$
971 concentration between inside and outside kelp forests – by rerunning the top LMM in Table S5
972 with the biomass of only one animal family at a time. We ran models for the 15 most abundant
973 families, but only present the three fish families (Gobiidae, Cottidae, and Hexagrammidae) and
974 three invertebrate families (Echinasteridae, Strongylocentrotidae, and Turbinidae) with the
975 highest $R^2$ values. These six families contribute almost half (44%) of the total biomass observed
976 on the surveys.

977 We found a negative relationship between $\Delta NH_4^+$ and the biomass of gobies (Gobiidae)
978 and evidence of a positive tide:goby biomass interaction (LMM, $p < 0.001$, Fig. S2.02). $\Delta NH_4^+$
979 was positively correlated with the biomass of sculpins (Cottidae; $p = 0.03$) and greenlings
980 (Hexagrammidae; $p < 0.001$), but no interactions with biomass were significant ($p > 0.32$). Sea
981 stars in the family Echinasteridae displayed a positive relationship with $\Delta NH_4^+$, a negative
982 kelp:sea star biomass interaction, and a positive tide:sea star biomass interaction ($p < 0.01$). We
983 found evidence for a smaller but still positive relationship between the biomass of urchins in the
984 family Strongylocentrotidae and snails in the family Turbinidae and $\Delta NH_4^+$ ($p < 0.02$), but no
985 interactions with biomass were significant ($p > 0.26$). Full model outputs are available in Table
986 S2.02.

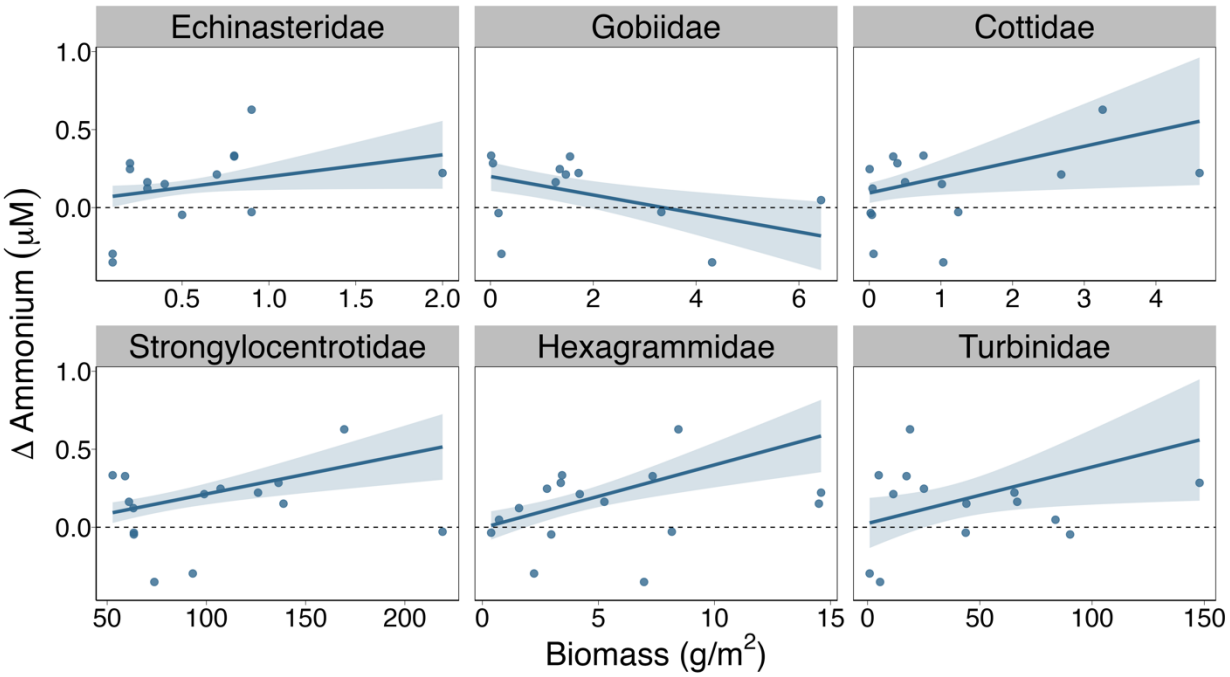


**Figure S2.02.** Model-generated predictions of difference in ammonium concentrations between inside and outside kelp forests in relation to animal biomass for the 6 animal families with the highest $R^2$.

993 **Table S2.02.** Model summaries from the small scale (within-site) models including only the
994 biomass of one family (indicated in the top left cell) for each model.
995

| **Echinasteridae** ($R^2$ = 0.96) | **Estimate** | **Std. error** | **z value** | **p value** |
|---|---|---|---|---|
| Intercept | 2.59 | 0.93 | 2.79 | 0.01 |
| Kelp - nereo | 0.26 | 0.05 | 5.52 | < 0.001 |
| Kelp - none | -0.06 | 0.09 | -0.60 | 0.55 |
| Kelp biomass | -3.47 | 1.21 | -2.87 | 0.004 |
| Tide exchange | 3.06 | 1.02 | 3.01 | 0.003 |
| Animal biomass | 5.87 | 2.19 | 2.68 | 0.01 |
| Biodiversity | -0.09 | 0.03 | -3.41 | < 0.001 |
| Depth | 0.03 | 0.02 | 1.02 | 0.31 |
| Kelp:tide | 0.20 | 0.05 | 3.91 | < 0.001 |
| Kelp:animals | -9.20 | 2.92 | -3.15 | 0.002 |
| Tide:animals | 7.02 | 2.39 | 2.93 | 0.003 |

996
997

| **Gobiidae** ($R^2$ = 0.92) | **Estimate** | **Std. error** | **z value** | **p value** |
|---|---|---|---|---|
| Intercept | -0.74 | 0.27 | -2.72 | 0.01 |
| Kelp - none | 0.81 | 0.35 | 2.29 | 0.02 |
| Kelp biomass | 0.70 | 0.42 | 1.67 | 0.09 |
| Tide exchange | 4.71 | 1.00 | 4.70 | < 0.001 |
| Animal biomass | -2.17 | 0.66 | -3.28 | 0.001 |
| Biodiversity | 0.13 | 0.04 | 3.45 | 0.001 |
| Depth | 0.002 | 0.03 | 0.07 | 0.94 |
| Kelp:tide | 0.12 | 0.09 | 1.31 | 0.19 |
| Kelp:animals | 1.74 | 1.05 | 1.66 | 0.10 |
| Tide:animals | 12.00 | 2.53 | 4.74 | < 0.001 |

998
999

| **Cottidae** ($R^2$ = 0.91) | **Estimate** | **Std. error** | **z value** | **p value** |
|---|---|---|---|---|
| Intercept | 1.54 | 0.66 | 2.35 | 0.02 |
| Kelp - nereo | 0.09 | 0.09 | 1.03 | 0.30 |
| Kelp - none | -0.45 | 0.10 | -4.53 | < 0.001 |
| Kelp biomass | -0.01 | 0.46 | -0.03 | 0.98 |
| Tide exchange | -0.16 | 1.35 | -0.12 | 0.91 |
| Animal biomass | 3.29 | 1.50 | 2.19 | 0.03 |
| Biodiversity | -0.14 | 0.04 | -3.89 | < 0.001 |
| Depth | 0.10 | 0.03 | 2.92 | 0.004 |
| Kelp:tide | 0.22 | 0.09 | 2.46 | 0.01 |
| Kelp:animals | -0.74 | 1.05 | -0.70 | 0.48 |
| Tide:animals | -0.64 | 3.18 | -0.20 | 0.84 |

| **Strongylocentrotidae** ($R^2$ = 0.90) | **Estimate** | **Std. error** | **z value** | **p value** |
|---|---|---|---|---|
| Intercept | -0.01 | 0.05 | -0.19 | 0.85 |
| Kelp - nereo | 0.06 | 0.08 | 0.82 | 0.41 |
| Kelp - none | -0.65 | 0.12 | -5.26 | < 0.001 |
| Kelp biomass | 0.19 | 0.05 | 3.53 | < 0.001 |
| Tide exchange | 0.07 | 0.06 | 1.02 | 0.31 |
| Animal biomass | 0.08 | 0.02 | 3.47 | 0.001 |
| Biodiversity | 0.04 | 0.03 | 1.34 | 0.18 |
| Depth | 0.09 | 0.03 | 3.09 | 0.002 |
| Kelp:tide | 0.14 | 0.06 | 2.40 | 0.02 |
| Kelp:animals | -0.01 | 0.01 | -0.87 | 0.38 |
| Tide:animals | -0.02 | 0.02 | -1.13 | 0.26 |

| **Hexagrammidae** ($R^2$ = 0.88) | **Estimate** | **Std. error** | **z value** | **p value** |
|---|---|---|---|---|
| Intercept | 0.57 | 0.12 | 4.97 | < 0.001 |
| Kelp - nereo | 0.06 | 0.09 | 0.67 | 0.50 |
| Kelp - none | -0.42 | 0.11 | -3.77 | < 0.001 |
| Kelp biomass | 0.45 | 0.17 | 2.69 | 0.01 |
| Tide exchange | -0.01 | 0.07 | -0.18 | 0.85 |
| Animal biomass | 1.33 | 0.34 | 3.89 | < 0.001 |
| Biodiversity | -0.08 | 0.03 | -2.71 | 0.01 |
| Depth | 0.01 | 0.03 | 0.44 | 0.66 |
| Kelp:tide | 0.26 | 0.08 | 3.36 | 0.001 |
| Kelp:animals | 0.48 | 0.48 | 0.99 | 0.32 |
| Tide:animals | -0.17 | 0.26 | -0.67 | 0.51 |

| **Turbinidae** ($R^2$ = 0.88) | **Estimate** | **Std. error** | **z value** | **p value** |
|---|---|---|---|---|
| Intercept | 0.04 | 0.07 | 0.50 | 0.61 |
| Kelp - nereo | 0.29 | 0.09 | 3.30 | 0.001 |
| Kelp - none | -0.34 | 0.21 | -1.60 | 0.11 |
| Kelp biomass | 0.23 | 0.05 | 4.30 | < 0.001 |
| Tide exchange | 0.02 | 0.05 | 0.35 | 0.73 |
| Animal biomass | 0.11 | 0.05 | 2.37 | 0.02 |
| Biodiversity | 0.09 | 0.04 | 2.27 | 0.02 |
| Depth | 0.01 | 0.03 | 0.40 | 0.69 |
| Kelp:tide | 0.21 | 0.09 | 2.37 | 0.02 |
| Kelp:animals | -0.01 | 0.05 | -0.17 | 0.87 |
| Tide:animals | 0.04 | 0.06 | 0.66 | 0.51 |